

Doctoral Thesis

Voltage Stability Management in Malaysia Power System with Inverter-Based Distributed Generator (インバータ連系型分散電源を含むマレーシアの電力系統における 電圧安定度管理手法)

Norhafiz Bin Salim
(ノルハフィズ ビン サリム)

Department of Physics, Electrical and Computer Engineering
Graduate School of Engineering
Yokohama National University

March 2017

Voltage Stability Management in Malaysia Power System with Inverter-Based Distributed Generator

(インバータ連系型分散電源を含むマレーシアの電力系統における電圧安定度管理手法)

by

Norhafiz Bin Salim

Dissertation submitted to the
Graduate School of Engineering of Yokohama National University
in partial fulfilment of the requirement for the degree of

Doctor of Engineering
in
Electrical and Computer Engineering

Supervisor: Professor Dr Takao TSUJI

Department of Physics, Electrical and Computer Engineering
Graduate School of Engineering
Yokohama National University

Yokohama, Japan

March 2017

ACKNOWLEDGEMENT

All praise, glory and gratitude be to Allah who said in the Holy Qur'an that "He who taught (the use of) the pen and taught the man that which he knew not". Peace be upon the Prophet Muhammad SAW, his family, his companions, and all those who followed him until the Day of Judgment.

First, I wish to express my deepest gratitude to my supervisor Prof. Takao Tsuji for the continuous support of my Ph.D. study and related research, for his personal attention, motivation, and immense knowledge. His guidance helped me in all the time of study and it was a great experience working and learning with him and without his enthusiastic support and interest, this thesis would not have been accomplished as here. It is such an honour to be one of his students through all the years.

Besides my supervisor, I would like to thank the rest of my thesis committee: Prof. Tsutomu Oyama, Prof. Atsuo Kawamura, Prof. Yasuka Fujimoto and Prof. Tomoyuki Shimono for their insightful comments and encouragement which incited me to strive more from various perspectives.

I am also indebted to Universiti Teknikal Malaysia Melaka (UTeM) for funding my doctorate study as well. Without the precious financial support, it would not be possible to complete this research.

My sincere appreciation also extends to all my lab mates and others who have aided at various occasions. Finally, special and deep thanks to my wonderful family especially to my beloved wife and kids for their tolerance and constant encouragement.

ABSTRACT

In many countries, past large-scale blackouts were caused by voltage instability phenomenon and it is of prime importance to enhance the voltage stability to realize stable power supply. At initial, sort of estimation approach using the artificial neural network (ANN) for a pre-defined solution in the real practical power system is discussed in the investigation with distributed generators (DG) participation. Next, this thesis presents a methodology to increase loading margin (LM) in terms of voltage stability by using reactive power support of DG, in particular photovoltaic (PV), considering the operating limits of power system components such as generators. The proposed method is based on optimal active and reactive power dispatch from DGs under normal and contingency conditions. Here, a trade-off relationship between reactive power injection and active power curtailment was carefully considered in optimizing the DG's contributions. The proposed method is based on Particle Swarm Optimization and its effectiveness was verified in Malaysian Electric Power System (MEPS) model along with constant power loads. It was observed through simulation results that optimal reactive power injection from DGs improved the maximum loading under the voltage stability constraint.

TABLE OF CONTENTS

CHAPTER	TITLE	PAGE
	ACKNOWLEDGMENTS	i
	ABSTRACT	ii
	TABLE OF CONTENTS	iii
	LIST OF FIGURES	vi
	LIST OF TABLES	viii
	LIST OF ABBREVIATIONS	ix
1	INTRODUCTION	1
	1.1 Research Background	1
	1.2 Problem Statement	6
	1.3 Research Objectives and Scope of Study	6
	1.4 Thesis Organization	8
2	DISTRIBUTED GENERATOR	10
	2.1 Introduction to Distributed Generator	10
	2.1.1 Inverter and Non-Inverter Based of DG	11
	2.2 DG Integration with Grid System	12
	2.2.1 Impact on Grid Stability	12
	2.2.2 Case Study	13
	2.2.3 Centralized Control	14
	2.2.4 Distributed Control	14
	2.3 Optimal Placement and Sizing of DG	15

2.4 Photovoltaic (PV)	18
2.4.1 PV Grid-Tie System	18
2.5 Solar Photovoltaic System in Malaysia	21
2.5.1 Potentiality of Solar PV in Peninsular Malaysia Grid	22
2.6 Summary	26
 3	
LOAD MARGIN ESTIMATION VIA ANN	27
3.1 Introduction	27
3.2 ANN Data Preparation	28
3.3 ANN Performance Criterion	31
3.4 Focused Time Delay Network	40
3.4.1 Tapped Delay Line (TDL)	42
3.4.2 Inter-Regional Power Transfer in Malaysia Topology	43
3.5 Summary	45
 4	
OPTIMIZATION FOR VOLTAGE STABILITY ENHANCEMENT	47
4.1 Introduction	47
4.2 Particle Swarm Optimization	49
4.3 Continuous Power Flow	53
4.4 Formulation for Normal Condition	54
4.5 Formulation for Contingency Condition	58
4.6 Supervisory Control Management	59
4.7 Summary	62

5	RESULTS AND DISCUSSION	63
5.1	Test System	63
5.2	Normal Condition	64
5.3	Contingency Condition	69
5.3.1	Case 2- Uniform Load Increase	71
5.3.2	Case 2- Single Load Increase with Heavy Load	76
5.3.3	Robustness of Proposed Method	79
5.4	Comparison of Single and Multi-Objectives Function	83
5.4.1	Comparison Analysis	84
5.5	Summary	88
6	CONCLUSIONS AND FUTURE WORK	89
6.1	Conclusion	89
6.2	Future Work	90
	LIST OF PUBLICATION	91-92
	REFERENCES	93
	APPENDICES	101

LIST OF FIGURES

Fig. 1.1. P-V Curve and Loading Margin with Reactive Power Support	2
Fig. 2.1. Percentage of Voltage Drops as a Function of Distance	17
Fig. 2.2. NEM Concept	19
Fig. 2.3. Solar PV System with Battery Connection	20
Fig. 2.4. Solar PV System without Battery Connection	20
Fig. 2.5. MEPS Network	22
Fig. 2.6. Daily Temperatures (a) Central (b) Northern (c) Eastern and (d) Southern	25
Fig. 3.1. Log-Sigmoid Activation Function	29
Fig. 3.2. Neural Network Structure Model	29
Fig. 3.3. Process of Computing Loading Margin	30
Fig. 3.4. Multi-Layer Perceptron Network Classification	32
Fig. 3.5. Radial Basis Function Network Classification	33
Fig. 3.6. (a) MLP (b) RBF Regression Plot	36
Fig. 3.7. (a) MLP (b) RBF Performance Plot of Error Convergence	37
Fig. 3.8. Voltage Profile at Weakest Bus	37
Fig. 3.9. (a) FTDN (b) DTN Layout	41
Fig. 3.10. Delay Line at Input Layer	42
Fig. 3.11. Inter-Regional Route Linkage in Malaysia Power System	43
Fig. 3.12. Comparison on Interface Flow Margin for Daily Basis via Neural Network Training and Testing	45
Fig. 4.1. Impact by PV Control on P-V Curve	49

Fig. 4.2. Graphical Illustration of PSO Velocity Components	51
Fig. 4.3. Flowchart of the PSO	52
Fig. 4.4. Feasible Region of DG Control under Apparent Power Limit	55
Fig. 4.5. Diagram of TSO Control Scheme for Contingency	61
Fig. 5.1. MEPS Network Model	64
Fig. 5.2. MEPS Load Curve	66
Fig. 5.3. MEPS Overall PV Generation Pattern	66
Fig. 5.4. Active Power Output of PVs via Proposed Method	67
Fig. 5.5. Reactive Power Output of PVs via Proposed Method	67
Fig. 5.6. Transmission Power Loss	68
Fig. 5.7. Voltage Profile in Normal Condition at 12:30	69
Fig. 5.8. Power Flow on Transmission Lines	70
Fig. 5.9. P-V Curve at Bus 15 (Case1 with Light Load)	72
Fig. 5.10. P-V Curve at Bus 16 (Case1 with Light Load)	72
Fig. 5.11. Voltage Profile at Stability Limit (Case1 with Light Load)	73
Fig. 5.12. P-V Curve at Bus 15 (Case1 with Heavy Load)	74
Fig. 5.13. P-V Curve at Bus 16 (Case1 with Heavy Load)	74
Fig. 5.14. Voltage Profile at Stability Limit (Case1 with Heavy Load)	75
Fig. 5.15. P-V Curve at Bus 15 (Case2 with Heavy Load)	76
Fig. 5.16. P-V Curve at Bus 16 (Case2 with Heavy Load)	77
Fig. 5.17. Voltage Profile at Stability Limit with Single Load Increase at Bus 15 (Case2 with Heavy Load)	77

Fig. 5.18. Loading Margin in Load Buses in Case 1 and 2	79
Fig. 5.19. Robustness Analysis of Fault Point	80
Fig. 5.20. Convergence Characteristic of PSO	82

LIST OF TABLES

Table 1.1	Annual Global Solar Radiation Average for Five Sites in Malaysia	23
Table 3.1	ANN Parameters	31
Table 3.2	Comparison between MLP and RBF Performances	34
Table 3.3	Comparison between CPF and MLP Performances	39
Table 3.4	Selected Line Outages	44
Table 5.1	PSO Parameters	64
Table 5.2	Optimal Solution for Normal Condition at 12:30	68
Table 5.3	Generation Capacity and Dispatch	70
Table 5.4	Optimal Solution in Case1 with Light Load	73
Table 5.5	Optimal Solution in Case 1 with Heavy Load	75
Table 5.6	Optimal Solution in Case2 with Heavy Load	78
Table 5.7	Loading Parameter Around Optimal Solution	78
Table 5.8	Validation of PSO Parameters	83
Table 5.9	Multi-Objectives Optimization	85
Table 5.10	Single Objective Optimization	87

LIST OF ABBREVIATIONS

LM – Loading Margin

DG – Distributed Generator

PV – Photovoltaic

RES – Renewable Energy Resources

STATCOM – Static Compensator

UPFC – Unified Power Flow Controller

PMU – Phasor Measurement Unit

OPF – Optimal Power Flow

ANN – Artificial Neural Network

TSO – transmission System Operator

TCSC – Thyristor Controlled Series Compensator

CPF – Continuous Power Flow

PSO – Particle Swarm Optimization

PCS – Power Conditioning Subsystem

MEPS – Malaysia Electrical Power System

NEM – Net Energy Metering

AC – Alternating Current

FiT – Feed-in-Tariff

MLP – Multilayer Perceptron

RBF – Radial Basis Function

RMSE – Root Mean Square Error

MSE – Mean Square Error

FTDN – Focused Time Delay Network

TDL – Time Delay Line

CHAPTER 1

INTRODUCTION

1.1 Research Background

Voltage stability often becomes a dominant constraint to determine maximum sending power in power systems. Because of the nonlinearity of power equation, the relationship between sending active power and voltage at receiving end is represented as P-V curve shown in Fig.1. Supposing that voltage characteristic of the load is modelled as constant power, the top of this curve becomes the stability limit at which the operating point turns into unstable. Here, the distance between this stability limit and the current operating point is defined as loading margin (LM) in this paper. Because this curve is shortened by faults on transmission lines, system operators have to carefully keep sufficient amount of LM considering the unpredicted fluctuation of loads in order to avoid voltage collapse.

The size of this curve also depends on the power factor of load, and it is possible to enlarge the curve, for example from solid curve to dotted one in Fig.1, by injecting the reactive power at receiving end. Namely, it is essential to maintain a proper balance of reactive power in power systems, and dispatch methods of reactive power among multiple synchronous generators have been studied with considerations of power factor constraint⁽¹⁾⁽²⁾⁽³⁾⁽⁴⁾⁽⁵⁾. Furthermore, deployment of tap-changers and reactive power compensators has been conventionally used to improve the voltage stability. Based on these ideas, advanced control methods to effectively realize the coordination between them have been developed so far⁽⁶⁾. However, many countries still experienced large-scale blackouts these days due to voltage stability issue. In (7)(8)(9), it was shown that maximum transfer

limit has become a primary concern at most utilities, especially transmission system operators, as inadequate reactive power support was a major factor in most of the blackouts. Hence, additional countermeasures should be required to reduce the risk of the voltage collapse.

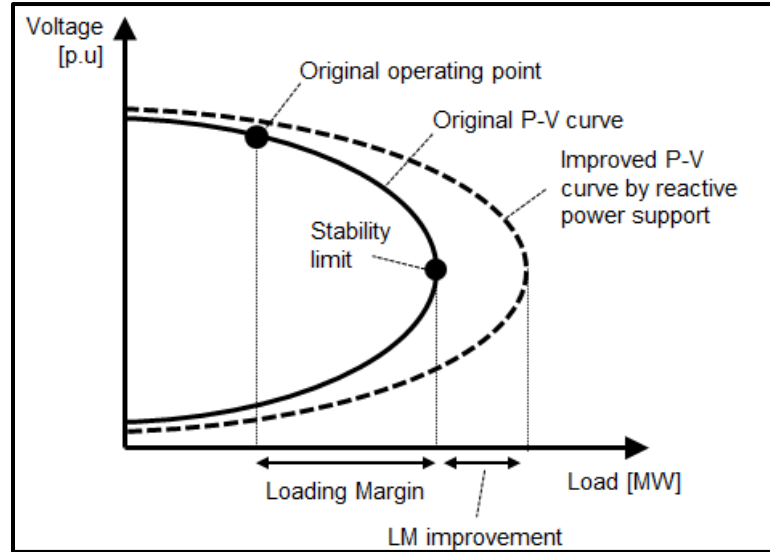


Fig. 1.1. P-V Curve and Loading Margin with Reactive Power Support

On the other hand, the penetration of distributed generators (DGs), in particular, renewable energy sources (RES) such as photovoltaic (PV) and wind power, is greatly increasing and growing in recent power systems. The renewable energy integration causes various issues because of their uncertain output fluctuation, for example, frequency regulation, loop power flow, voltage fluctuation and so on. However, DGs can also contribute to stabilizing power system operation and control by using their active and reactive power controllability. For example, the effectiveness of PV control on voltage profile or power loss has been studied in (10) and (11). Also, in (12), with DG employment in the power network, optimal reactive power control has been presented by using centralized voltage control scheme while keeping a thermal limit of system branches. In (13), an attempt to optimally utilize reactive power control of DG is investigated to satisfy a number of requirement i.e.

allowable voltage regulation and capacity of DG. Similarly, it is expected that reactive power control from a lot of PVs can improve the voltage stability issue⁽¹⁴⁾. Hence, the main purpose of this study is to develop a new control scheme for LM maximization by using reactive power control of PV plants.

There are two ways to control DGs: centralized and decentralized methods. For example, in (15)(16)(17), centralized operation methods were proposed by solving network optimal power flow with regard to minimizing line and inverter losses. Meanwhile, in decentralized approach⁽¹⁸⁾, control action of each DG was determined by local information with less communication apparently. In general, a centralized method is superior in optimizing objective function more strictly while decentralized method has better control speed with light computation burden⁽¹⁹⁾. The proposed method in this paper is mainly based on the centralized approach. Because the optimization problem often becomes complex formulation with large scale, various calculation techniques such as linear programming⁽²⁰⁾, gradient method, interior point method⁽²¹⁾ and computational intelligence algorithms⁽²²⁾ have been applied in the field of the power system in order to obtain the solution more efficiently.

There are various past studies related to LM management or voltage stability issues. For example, in (23) -(26), the improvement of maximization of LM was discussed even though without any deployment of DGs which could bring more complexity as well. In (23), (24), and (25), various control method for LM improvement was developed with the presence of static var compensator (SVC), online line switching, and other reactive power sources. In (26) and (27) a UPFC and STATCOM have been determined for its best positioned and setting and by applying multi-objective formulation in which to minimize investment cost, transient voltage and proximity to voltage collapse. In addition, the control scheme consisting of preventive and corrective controls with load curtailment was proposed in (24). Also, LM was considered in economic load dispatch mechanism in (28).

On the other hand, there are many papers about estimation or evaluation methods of LM. In (29), a hybrid mechanism of genetic algorithm with neural network approaches was incorporated together in order to have the best accuracy, the speed of calculation and operational wise on LM estimation. Meanwhile, in (30), maximum loading point was determined purely with having bisection searches between feasible and infeasible load flow cases. In addition, the application of phasor measurement unit (PMU), a new optimal power flow (OPF) considering stability index about voltage collapse, and a new stochastic calculation method of LM were developed in (31), (32), and (33), respectively. In these papers, however, the existence of DGs had not been considered yet.

Thus, in a bigger picture relating to LM insights, after all, it is straightly connected to the voltage stability reinforcement from every angle of perspective for example attachment of variation of compensation devices, reactive power controllability, active power reduction, and even the introduction of distribution generators. Many ways of contemplating for voltage stabilisation mechanism so manifestly each approach would be detrimental from one to another if the controllability and reliability between them and the grid system are not content and well-maintained. In (34) and (35) only discussed loading margin improvement using a continuation method and fast algorithm with real power losses reduction to tracing stability margin. The comparison has been made with optimal power flow and shows better performance in term of voltage stability. Commonly for ensuring voltage stability is not vulnerable the online monitoring generally proposed ⁽³⁶⁾ under normal condition and also contingencies with applying various kind of numerical method i.e. ANN. For example, in (37), a mechanism of strategic online line switching is applied to yields high-quality solutions while screening, ranking and identifying the power system. Operation. Basically, this proposed approach trying to offer opts for TSO to ensure load margins would be enhanced with technically pre-evaluation of look-ahead power stability. Sometimes reliability of metaheuristic approach can be vigorous or susceptible in governing dynamic phenomenon of voltage stability thus as in (38) two optimization been deployed in steps for finding an optimal location for Thyristor Controlled Series Compensator (TCSC) with Improved Search

Gravitational Algorithm (IGSA) and improve voltage stability and cost sizing via Firefly Algorithm (FA) respectively. In the end, all the results being compared to seek whichever could yield better performance without contemplating overloading margin issues. Hence, dependency towards conventional generators must not take lightly because with effective coordination of thermal generators they could possibly synergize their outputs to improve short-term voltage stability. Moreover, the reactive power can be controlled at the high-side which consist of multimachine Var coordinator and voltage controllers to intensifying voltage support and load margin ⁽³⁹⁾.

At glance, it is noticeable that participation of renewable energy resources seems limited when discussion of loading margin towards voltage stability is brought up in in previous academic investigation. However, yet some discussions have been done to uptake with the potentiality of these free natural energy in extracting active power whilst adopting optimization tools ⁽⁴⁰⁾. In (41) although there is a deployment of stochastic of wind power for voltage control correction but economic cost control must be also embedded along with demand response participation. Specifically, the optimization is more to reduce the operation control cost such a way to achieve desirable loading margin without considering reactive power control reinforcement. As in (42) a simplified probabilistic voltage stability using two-point estimation and continuous power flow (CPF) for voltage stability was evaluated. In this investigation, both solar and wind power have been a model for determining the voltage stability acquisition. The deeper investigation should be applied for the uncertainty analysis of renewable energy to guarantee system reliability. Hence kind of voltage stability index with considering typical load models should be appointed eventually with can be applicable for any kinds of topology i.e. grid connected or islanded mode. In (43) combination aimed at enhancing power loss minimization and system frequency deviation have been considered thoroughly with the unstable wind power penetration.

1.2 Problem Statement

Presently, there are less number of papers in which the existence of DGs is considered in LM issues. In (44), voltage stability assessment was focused considering wind power plants by using V-Q sensitivity. Also, in (45), LM assessment method was proposed considering renewable energy sources based on neuro-fuzzy logic. However, the contribution of DGs to LM maximisation has not been developed yet in these papers. Therefore, a comprehensive study needs to be investigated the impact of DGs especially solar PV on loading margin assessment. In addition, although there is numerous strategy to properly allocated DGs in the network for instance via heuristic method but likely active power curtailment is not treated as a constraint in previous papers problem formulation too.

Hence, in this paper, we focused on an optimal control method of PV plants in terms of normal and contingency conditions without using any modern reactive power control equipment as mentioned previously. Here, the main purpose of the optimization is to maximize LM maximization under contingency condition. The operating points of PV plants are determined using Particle Swarm Optimization (PSO) with considering trade-off relationship between active and reactive power control under current limit of Power Conditioning Subsystem (PCS) of PV plants. Although the proposed method is based on the centralized method, its robustness against fault point is verified in order to use the optimal solution which was obtained in advance right after the fault occurs as a decentralized approach.

1.3 Research Objectives and Scope of Study

The main objectives of this research are to evaluate and validate the impact of PV plants on voltage stability and develop a kind of strategy to dispatch reactive power control regarding active power curtailment considering apparent load demand. In all, the targeted aims of this investigation are explained as follows:

- i. LM maximization is realized by optimization technique where active and reactive power control of PV plants are treated as deterministic variables.
- ii. Reactive power control of PV plant is in general effective to improve LM. However, there is a possibility that LM deteriorates by excess reactive power supply inversely if active power curtailment is required due to the limitation of power conditioning subsystem (PCS) capacity because the apparent demand of load buses might be increased by the curtailment. This trade-off relationship is carefully treated in this paper with considering both active and reactive power control of PCS.

In addition, the optimal operating point is derived not only from contingency condition but also normal condition. By comparing these solutions, the importance of changing operating point in contingency condition will be shown.

At the early stage in this research load margin estimation with using CPF and Artificial Neural Network (ANN) were endeavoured to assist with brisk power system operation alongside contingency scenarios. Generally, this is very useful as for planning phase but to further benefit in voltage stability vicinity, not only preventive plan should be deployed but the corrective plan must be inserted too. In spite, however of ANN splendid preventive approach, yet another strategic corrective procedure is necessarily required to verify solar PV plants performance whilst being integrated into the utility system.

Thus, in the second part which is the core of the investigation was discussed, the solar PV plants are deployed into Malaysia Electric Power System (MEPS) for LM enhancement. Ever since wind power capacity is not so prominent and reliable up to the date of the country it is disregard completely indeed. Three locations have been finalized through optimization to set their optimal location with 7 generators on 17 bus system. All the performances are carried out and validated using PSO and CPF techniques via MATLAB environment.

1.5 Thesis Organisation

This thesis is organized into six chapters. The next following five chapters of this thesis are arranged as follows:

Generally, in Chapter 2 introduction to Distributed Generators are described. The effect of DG contribution on power system namely voltage stability is highlighted with a sample of the case study. The capacity and sizing of DG deployed to the grid is also presented. A glance of DG provision and application in Malaysia power system is discussed in this chapter too.

Chapter 3 presents the use of intelligence system namely artificial neural network (ANN) with CPF to estimate the load margin for real online system. All the inputs of the generations, demands and solar power for Malaysia power system were embedded together and being modelled using the MATLAB program. Simulations were carried out by supposing this attempt would delineate and set forth manifestations of a subsequent decision by the system operator in adhering system stability literally.

Chapter 4 expounds the application of optimization method for determining the optimal placement and amount of active and reactive power of PCS capacity with regard to load margin improvement in normal and contingency events. Here, a multiobjective formulation is dedicated to solving the integration problems for minimizing system loss, voltage deviation, and active power curtailment respectively. Furthermore, a comparison using single objective with multi-objective optimization were presented to elucidate and perceive execution of the parameters involved in the investigation.

Chapter 5 discussed the overall results in conjunction with load margin enhancement yielded from proper DGs enforcement towards achieving voltage stabilization especially during disturbances. Lastly, in Chapter 6 it concludes the significant contribution of this study

and further suggest kind of future work which can be incorporated so as to intensify existing achievement.

CHAPTER 2

DISTRIBUTED GENERATOR

2.1 Introduction to Distributed Generation (DG)

The increase in oil and natural gas price were inevitable over the past few years has encouraged many engineers, economists, and researchers to look for other energy resources. Distributed generation is a flexible technology that considerably not a new concept but currently receiving decent attention as power industry's stakeholders begin to take a big turn in their business practices by investing enormous money and effort to meet with trending electric energy business eventually. Wind energy and solar energy have recently being introduced in a large scale composition into the power network. One of the important factors of these alternative energies is to sustain its penetration level and reliability. Currently, our view still has a prioritization focus onto security at the first place with affordability following close behind making sustainability at the third but this ordinary mind setting going to be changed not gradually but seems swiftly. Over these past few years, considerable researches and development works have been devoted to the ancillary equipment and also related accessibility factors.

Specifically, promoting of solar energy utilization for enhancing power system transmission has become a fad in many countries either in economic or security approached. This was intensified by a mechanism so-called feed-in-tariff (FiT) to facilitate the growth of the green technology industry and enhance its contribution towards economic development. Globally, the PV solar cost is still very high compared to thermal and wind power however

with new upcoming modification of new materials, manufacturing process and the improvement of system converting efficiency, the cost of PV generations going to decrease steadily. The substantial pace of PV growth can be seen recently in Asian countries especially China and Japan which elucidate their target to achieve around 270 GW and 53 GW respectively by 2030. However, meticulous action needs to be refined if large penetration of solar PV will be available in near future because once the penetration number of solar PV plant goes any higher, adversely affected voltage profile becoming unpredictable and unstable. In addition, as certain to happen reverse power flows in the system will worsen the situation if brisk and decent curtailment is not realized. Commonly, voltage stability issue is the biggest threat in a power system distribution and transmission whereby it can be categorized into 3 aspects which are a voltage drop, voltage swell, transient, and interruptions; with estimated percentage number of 60%, 29%, 8% and 3% respectively (46). When the challenges of DG interconnection into the grid is completely ready e.g. stability, the existing power system can now be retrofitted with sort of power electronic devices to meet the new performance specifications in the system such as the converters. The direct current (DC) of DGs must be changed to alternating current (AC) enabling them for supplying and injecting the power into the main utility grid. Namely, there are two kinds of DG which are inverter-based DG e.g. PV and WT and non-inverter based DG e.g. mini hydro power being connected to the system grid worldwide.

2.1.1 Inverter and Non-Inverter Based of DG

Typically an inverter converts DC voltage and current into AC voltage and current by using power electronics equipment. This inverter will automatically synchronize grid voltage and frequency and likewise can be used for power factor correction hence providing substantial flexibility compared to non-inverter systems. Basically, for non-inverter technology, the speed of the engine is required to force a synchronous generator or induction generator to deliver desired AC power frequency. In fact, mostly this non-inverter DG depend on supplied fuel to allow then operated efficiently which is completely not required as in

photovoltaic and wind energy. Inverters work by taking the DC power from the photovoltaic modules and inverting it to AC power so it can be injected into the grid. Few names of an inverter that are available in the market are the micro inverter, string inverter, and a central inverter which categorized typically to their size and scale of installation respectively. Energy storage system is not required or can be unprioritized in larger power system with grid tie deployment provided the utility power is reliable and well maintained. In the event of a blackout, it must be assured that grid tie inverter will disconnect briskly regarding NEC requirement and to avoid any other potential harming occurrence on the grid.

2.2 DG Integration with Grid System

2.2.1 Impact on Grid Stability

To ensure power system stability, it is prime importance to match the generations with all the demands at most of the times. Integration of any distributed energy resources (DER) or DG will be treated as a form of additional generating power which mainly located near the load sides. Conventional existing generators at the transmission level are modelled explicitly in power flow and stability studies adopted in planning and designing phase for electrical power systems in static analysis by then utilized to determine and maintain the system operation. Hereby, DG participation must undergo similar analysis assessment likewise for ensuring grid stabilization. If the balance between generations and demands is not maintained, voltage collapse or knowingly blackout events could happen. In addition, manifestly the oscillation occurrences due to abrupt changes in generation or demand should be compensated quickly to prevent cascading outages with available compensating ancillary devices. However, it can be possible that reinforcement from these devices would be insufficient and alternative action must be taken. Moreover, acquisition of deterministic information of grid status under balance condition such generator's capacity, voltage profile's magnitude and thermal limit of transformers and transmission lines will be more meaningful for stability possession too.

So, to avoid this problem it is strongly supposing that DG i.e. solar PV plants must be deployed to yield further enforcement with controlling its output power optimally and help to embrace grid stability and most important can remain connected to the grid during a short period of faults thus allowing fault ride through phenomenon. Practically any relevant parameters will undergo changing process once they experienced disturbances and contingencies during online operation which presumably it can offset deliberately with a pragmatic approach. Thus in the nowadays modern power system, interaction and communication between existing conventional generating plants and PV plants can be controlled via two ways either in centralized or decentralized mode depending on the purposes and targeted control.

2.2.2 Case Study

In here (47), a comparative investigation of solar PV effect on system stability at different penetration levels with three different scenarios are studied: i- distributed PV, ii- centralized PV with and without voltage regulation capabilities. Real network data of Ontario, Canada was chosen to further yields impact of the eigenvalue, voltage stability, and transient stability. As presented in the study, a model of Ontario's transmission network was used to carry out the assessment. It was reported few feature in this model such as the lengthy distance of generator units in the north which comprises hydro generations, highly demand in the south mainly supplied with nuclear power. Due to this characteristic, the connection between west and east of the system tend to oscillate which then require system stabilizers at selected generating units. This investigation substantially important and likewise can be discussed and adopted using the equivalent model of Malaysia power system in the next chapter.

To that end, it was summarized that there is no significant effect using solar PV over small-signal stability. Conversely, it was determined and verified that distributed solar PV improves system stability for voltage and transient studies as compared to centralized solar PV. This can be true since with inclusion of neighbouring interconnections the existing committed

resources and facilities correspond to the system behaviour once solar PV being deployed into them.

2.2.3 Centralized Control

When a particular type of energy is dispatched to distinct consumers under the centralized administrative system it is called centralized system. In choosing what kind of best mode of operation control of DG it comes down to a number of factors but primarily from the wide perspective the total cost and energy production will be contemplated. In general, centralized control architecture provides the best cost of operation since its only involved central inverters. It is common this kind of control being adapted for larger scale of utility projects and commercial due to its low capital cost efficiencies. Despite the economic wise of this strategy which had become particularly noticeable since last few decades, it must be realized with massive increment of power market players with sort of renewable energy resources at hands it is now leading the world towards new perspective of power and energy management in becoming more realistic and businesslike thus a need on paradigm shift will likely emerge and expedited tremendously.

2.2.4 Distributed Control

Distributed control refers to the controller elements which are not central in location but are distributed throughout the system with each components sub-system being controlled by one or more controllers. Mitigation of disturbances or faults in a power system is so crucial not only during stable operation but also in a dynamical manner. With centralized control option, usually, network control action seems bit lag due to the limitation of communication speed which appears one of the bottlenecks in an online power system operation. However, this can be overcome by introducing distributed control action as the control is extremely fast due to its closer distance to the loads and autonomously. Preferably this kind of control it involves a small and medium scale of operation, unlike centralized control. In the view of

power utility this strategy undoubtedly so realistic, although first-cost efficiencies are not promising and decent, because as the functional capabilities of this control rapidly increase, it is likely that more investment and accommodation will move up to enabling the energy production sector towards global open market mechanisms with more involvement from aggregated users. In certain cases, a centralized control could be a better choice in smaller scale system, while distributed control could be optimal for a larger scale system but the bottom line is that the one that can provide better reliability and usability to uphold stochastic behavior in power system enthusiastically should be chosen with regard to any constraints. Long transmission lines are one of the main causes for electrical losses thus with distributed control it leads to energy efficiency emphasizing provided it must be the best location and yields tolerable amount of required injection upon commitment.

2.3 Optimal Placement and Sizing of DG

The feasibility of DG utilization will keep on growing for grid connected applications worldwide. This feature can be very vital in reducing system congestion and power system losses however, power system utilities need to adopt conservative limits of how much capacity of DG can be installed and at the same time would not bring any harm and negative impact to the power system. If the DG outputs are larger than the inverter's nominal power output than the inverter must reduce the output according to its nominal power and if DG outputs are lower than the inverter's nominal power, inefficient operation by the inverter will happen. From a viewpoint of voltage aspect, a damage to the inverter is unavoidable if the harvested voltage goes beyond maximum operating point's boundary which likely leads to system failure eventually. In order to avoid any serious problem e.g voltage rise, a need for refining alternative can be addressed in general as follows:

- i. Reduce the secondary low voltage transformer voltage.
- ii. Increase conductor size or reducing line impedance.
- iii. Curtail active power from DG.

The first two alternatives can be treated as an ordinary resolution which is a dominant response or operation-based from the system operator. Indeed, the intermittent nature of DG e.g. WT and solar PV make the system stability control at a big stake and if it goes to high, power reduction namely active power curtailment cannot be avoided which requires complex coordination and communication among all the DGs.

Apart from above-mentioned resolution, another reliability factor that can mitigate the impact of surplus power from DG is by optimizing the installed location. Some can deduce that any DG participation must be deployed to the highest load demand but this is untrue for some occasion since diversification and disruption in existing power system is unpredictable. Presently most DG sites are located closely to the load demand to eliminate power loss and minimize voltage reduction at the point of connection as shown in Figure 2. It is pre-requisite for the utilities to perform feasibility analysis in general before installing DGs. Commonly DG owner is required to decide the type, size and location of DG prior application to the responsible utility. In fact, in some cases, even DG has been optimally placed and sized but to retain and prolong its resilience can be somehow unprecedented. Commonly there are two factors could impact PV facilities which are temperature and amount of insolation level seasonally or regionally but these can be treated as external constraints or regular intermittency phenomenon.

So, there are some studies that applied few methods to find the best placement and sizing using analytical and optimization alternatives for solving these complicated problems. In (35) it reduces the use of global search to increase the speed of searching in PSO environment to reduce system losses while searching the best location of DG. Meanwhile, the results are compared with analytical method (AM) and grid search algorithm (GSA) and it seems from the results they work equivalently. In (48) a different kind of DG is implemented with using analytical method for three and four number of DG. It is reported that loss reduction is better with static load compared to the dynamic load. Some study has described on sensitivity factor of active power loss (LSF) to determine the most sensitive

buses for DG placement but it is understandably it is common that the weakest buses should be prioritized for DGs attachment to avoid more severe instability to happen at adjacent buses. Undeniable these DGs participation offer great enhancement in power systems but from this study which taken by a company claiming that not only the placement and size are concerned but also their generated power contract price. Thus, here in (49) utilization of multi-objectives PSO (MOPSO) has been used to solve the problem and simultaneously reducing power loss and improve grid reliability.

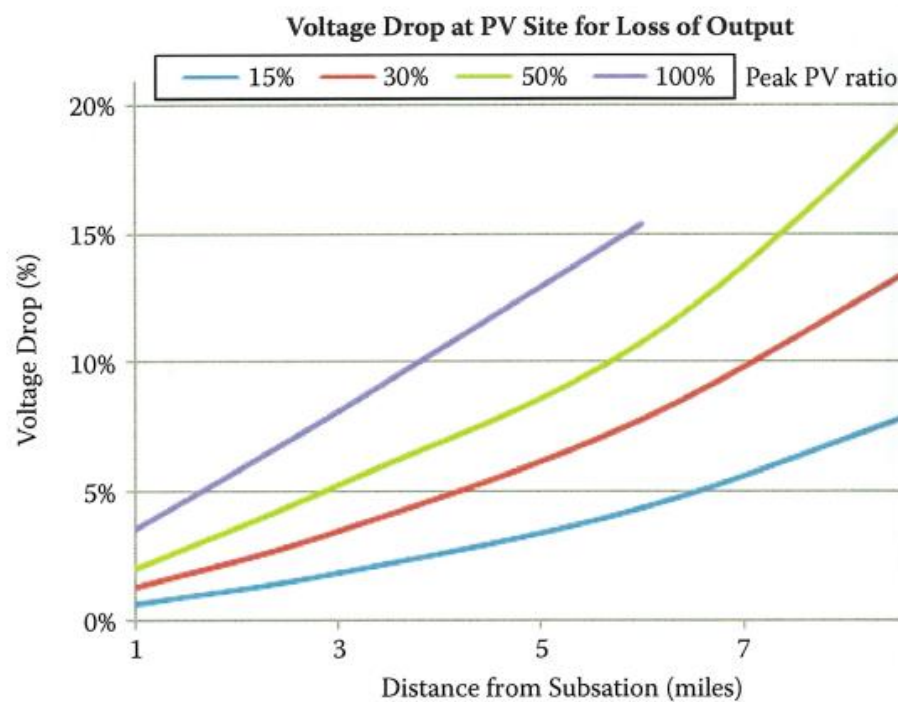


Fig. 2.1. Percentage of Voltage Drops as a Function of Distance (50)

2.4 Photovoltaic (PV)

2.4.1 PV Grid-Tie System

Electricity generated by solar PV plants need to be transmitted to the areas of consumption. Therefore, a PV grid-tie system is an essential factor to be concentrated allowing them to be interacting with the utility, with or without batteries configuration. As such, a storage system is basically absent in large grid-connected networks due to cost effectiveness and maintenance as compared to stand alone power system. Depending on each country before installing this system, it must be permissible by the utility for allowing users connection of the solar system to their electrical grid. Ideally, any surplus energy from the owner can be sold to the utility at the same retail rate of general electricity and this is known as a net metering system. As the worldwide cost of solar PV system gradually to fall each year, the energy consumer can benefit via this net metering scheme with producing their own energy from the own place. This is not only limited to the domestic user but also available for commercial and industrial sectors as long as they engaged to the actively responsible utility. The concept of net energy metering (NEM) in Malaysia has been launched which complement the Feed-in tariff (FiT) mechanism and could further contribute to achieving the national RE target and put less dependency on fossil fuels in future.

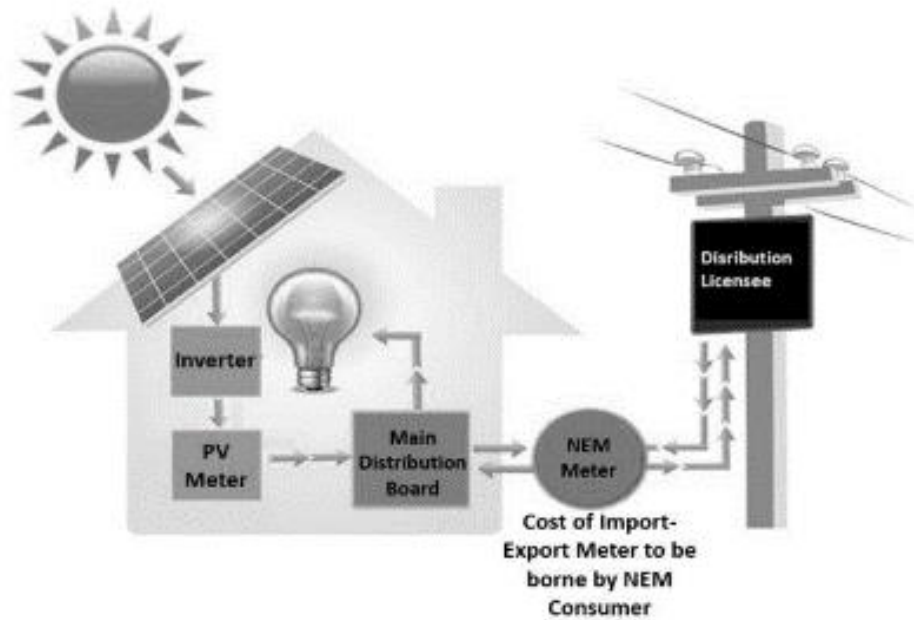


Fig. 2.2. NEM Concept (51)

So after getting the accessibility to the main grid interconnection, consumers need to figure out what will be the ample capacity of the installed system will work the best. The decisive action for this problem notably lies on the location for capturing the solar irradiance as more haversment will yield more power to the grid which by then being stored using energy storage system for example battery and later uses as a backup power. In a nutshell, optimal placement and the capacity of DGs participation absolutely play an extensive role in the aspect of technical and economical impact.

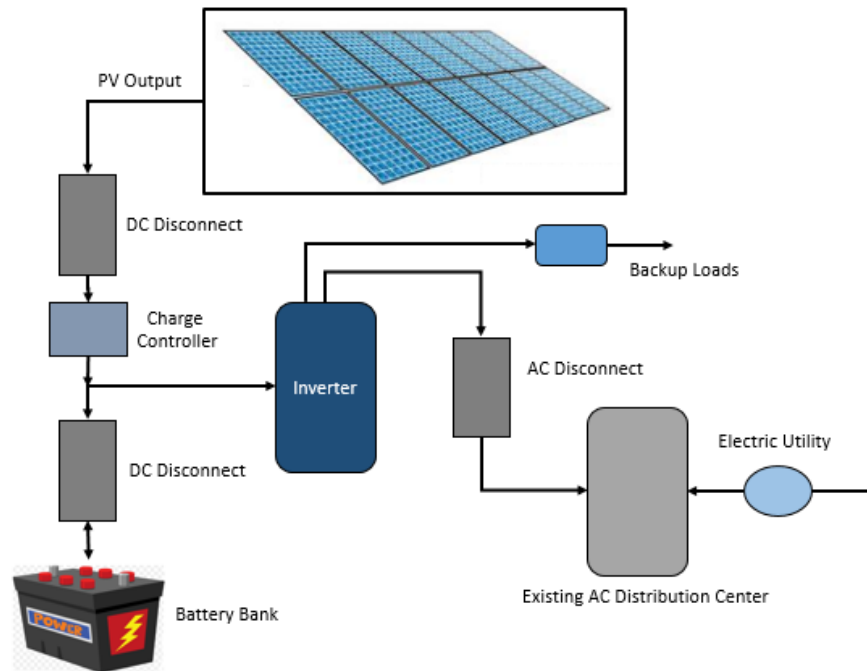


Fig. 2.3. Solar PV System with Battery Connection

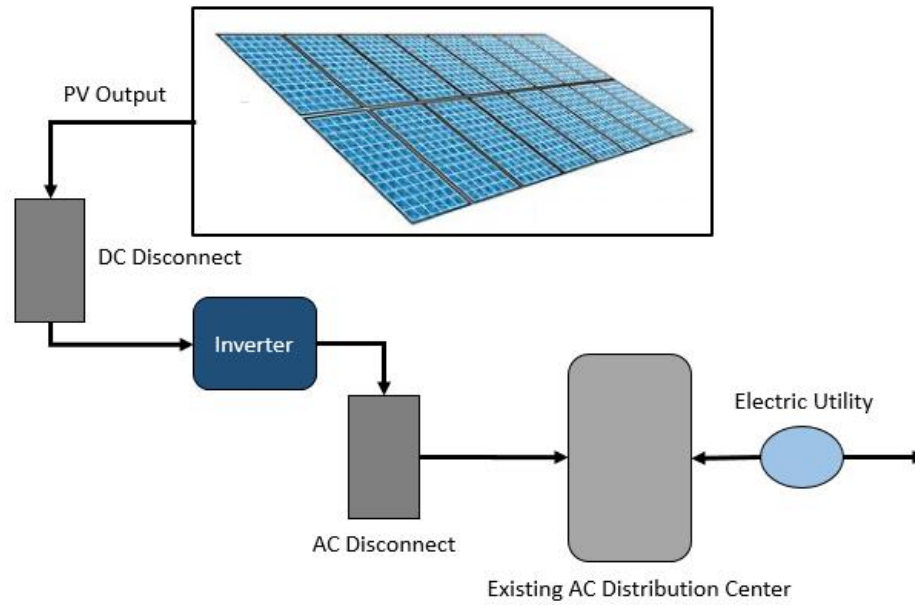


Fig. 2.4. Solar PV System without Battery Connection

2.5 Solar Photovoltaic (PV) System in Malaysia

Presently, the country had addressed latest PV market and PV policy development and come out with a strategic vision which will lead to competitiveness and greater control in the local market. The program is currently being conducted by Industry Development Program (IDP) and supporting Malaysia Building Integrated Photovoltaic Project (MBIPV) which to be realized in near future. However, there are few challenges need to take into consideration been enlisted to urge the program as follows (52):

- i. Capacity building for local industry to improve their capabilities
- ii. Enhancement in quality of manufacturing
- iii. Enhancing service, including after-sales and maintenance
- iv. Government incentive to drive the market and create competitiveness against global players

It has been reported that from 2001, the country has experimented with RE policy focusing on market forces to deliver and treat RE as prime energy for electricity generation. In 2009, a new effective policy is re-designed to address few constraints such as arbitrary price setting, lack of regulatory framework and less of institutional measures. Thus a new proposed forward-looking RE policy are listed as below (53):

- i. To increase RE contribution in the national power generation mix
- ii. To facilitate the growth of the RE industry
- iii. To ensure reasonable RE generation costs
- iv. To conserve the environment for future generation
- v. To enhance awareness of the role and importance of RE

2.5.1 Potentiality of Solar PV in Peninsular Malaysia Grid

In this investigation, there are four potential regions to locate DGs which are the northern, eastern, southern and central area. Each of these areas has a different aspect of generation and demand behaviour for instance in central region supply and demand balance is almost equal with most generation powered up by the thermal power plant and gas turbines while in the northern part, hydropower is scattered with few of thermal generations. Currently, it is expected probably more load growth in the western region in near future which indicates more secure power transfer among regions and additional reactive power compensation at the point of connection indisputably are needed. Demand in eastern area is not so congested but with a huge amount of thermal power generation in there it is necessary to dispatch the power out and supply to other regions. By given all these elements, it will be more challenging to scattered solar PV into the grid system so refine planning of the topology aspect beforehand should be studied and investigated as shown in Fig.6 below.



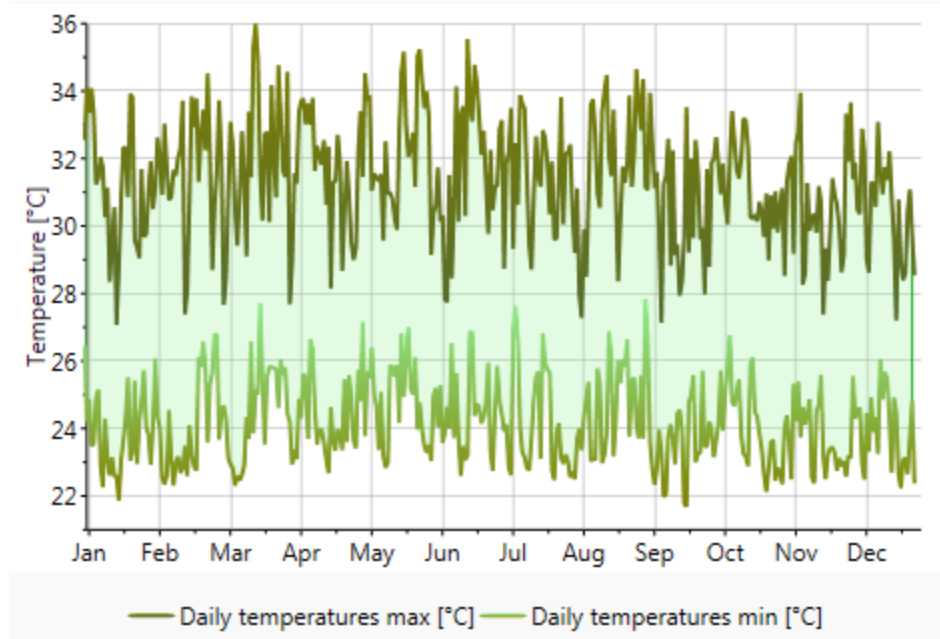
Fig. 2.5. MEPS Network

Basically, error evaluation of solar irradiation must be determined from measured and forecast readings per any time interval. For examples in Japanese power system for 8 hours of the interval, the average error value is 9 % and maximum at 22 % and these reading are the best deviation rate by far with given recent achievement in technological and efficiency of the technical systems (54). Insolation levels could change its output throughout the year, lowest in winter and highest in summer for instance. So as matter of fact, a hot desert could give a reading of 7 kWh/m²/day so it can be accessed for Malaysia and presumably to have an average of 4-5 kWh/m² with given tropical climate over the months. This can be shown as in Table 1 below.

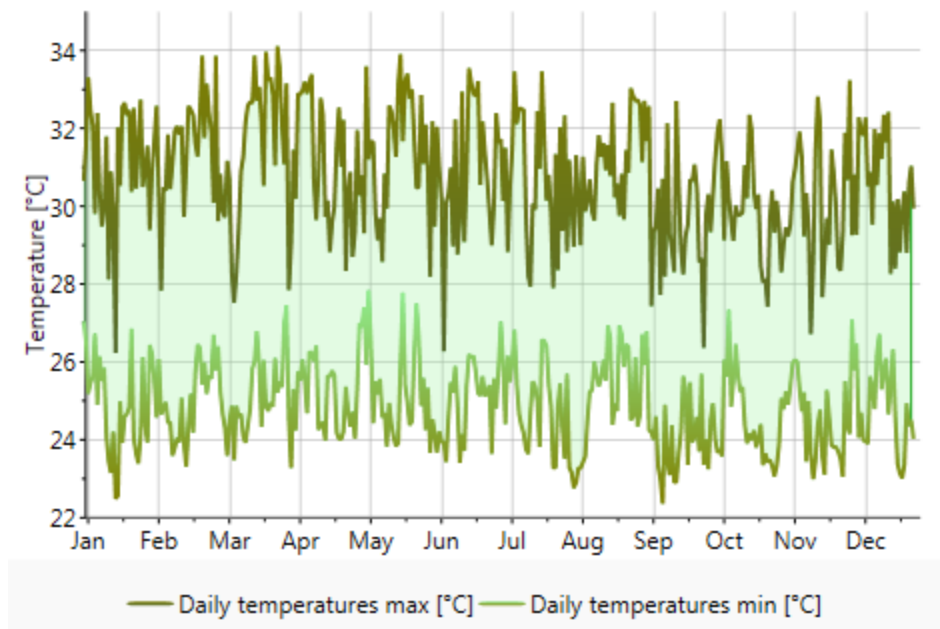
Table 1.1: Annual Global Solar Radiation Average for Five Sites in Malaysia (55)

Site	Average Measured (kWh/m ²)	Average Predicted (kWh/m ²)	Deviation (%)
Kuala Lumpur	4.84	4.83	0.20
Johor Bahru	4.51	4.55	0.89
Ipoh	4.54	4.64	2.20
Alor Setar	4.66	4.8	4.72
Kuching	4.62	4.66	0.86

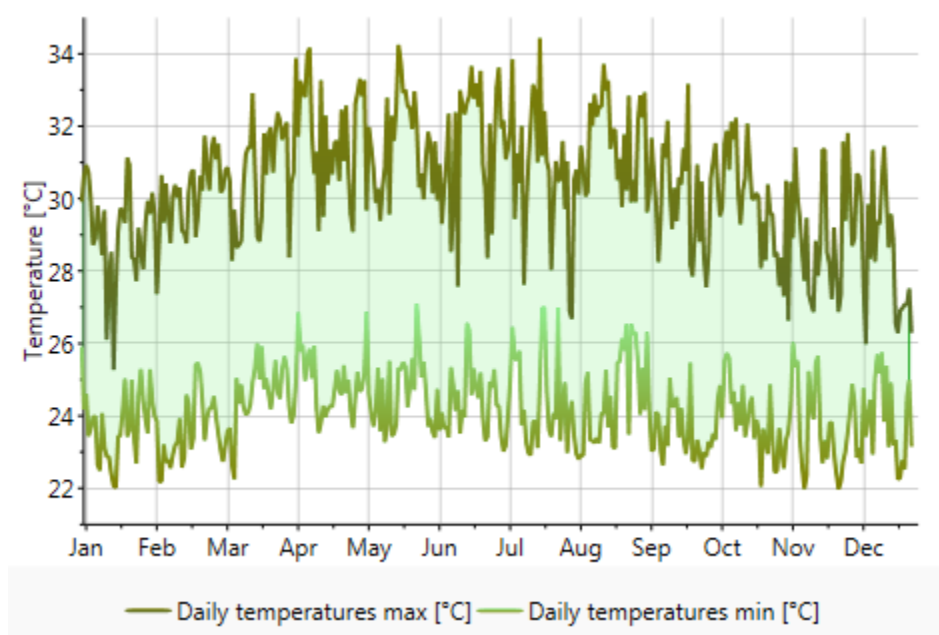
It has been notified that there are 4 sites in Malaysia been tagged by one of comprehensive meteorological reference from Swiss database. Four of this location are Kuala Lumpur, Penang, Kelantan and Johor which each one of them considerably would present specific region in typical for Central, North, Eastern and Southern regions respectively. The further extensive detail in each site can be roughly illustrated in next following Figures 7.



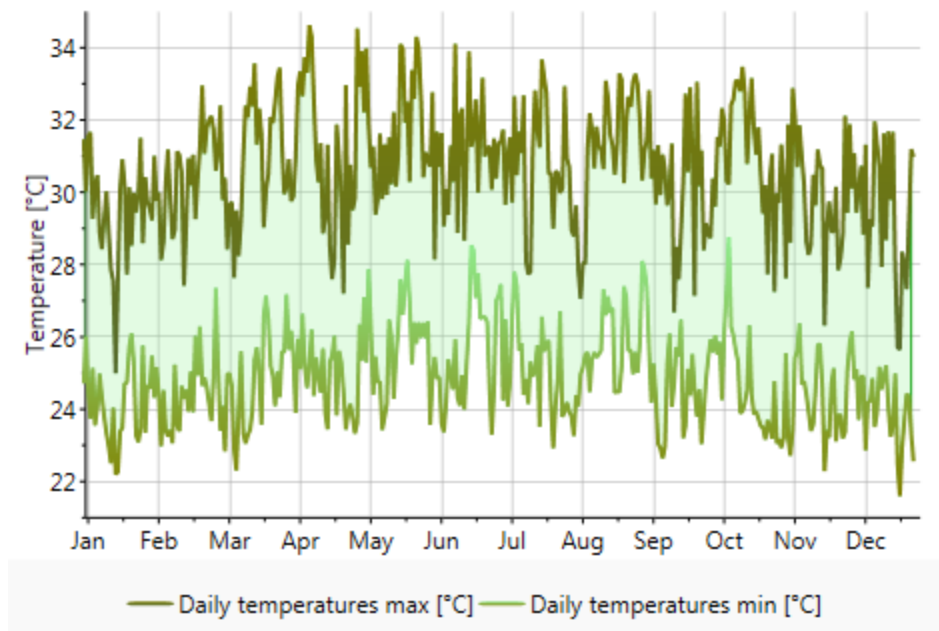
(a)



(b)



(c)



(d)

Fig. 2.6. Daily Temperatures (a) Central (b) Northern (c) Eastern and (d) Southern

From above figures, vividly the country only experienced sunny and rainy seasons within 12 months, unlike other four seasons countries. This is what make Malaysia have a very good potential for harvesting more solar irradiation and generating electricity from this natural energy resources and likewise making a prediction and forecasting of its contribution for any applied time interval feasibly astonished.

2.6 Summary

This chapter explained on distributed generators overview and its impact on the power systems. Even though a general description on DG is presented but later in the next chapter to be specific only solar PV plants will be used for deeper investigation. There are such many controls mechanism and strategy on the various perspective of DG approach with regard to stability analysis e.g. voltage control. In this thesis, the heuristic method based on PSO is proposed for determining the trade-off between the active and reactive power of not only DG capacity but also placement as a blueprint for load margin enhancement with regard to voltage stability issue.

CHAPTER 3

LOAD MARGIN ESTIMATION VIA ARTIFICIAL NEURAL NETWORK

3.1 Introduction

The continuation algorithm has substantially been utilized largely to discover a path of composite solutions of a set of nonlinear equations. From this conception, this continuation power flow (CPF) will be able to find a continuation solution for a given load change scenario with implemented general principle whilst employs a predictor and corrector scheme to track on a feasible solution. More detail explanation on this will be discussed later in the next section. Here, Artificial Neural Network is presented for estimating load margin with CPF. In fact, this presented method is capable too of obtaining power transfer limit between regions for real online monitoring purposes. In addition, there are several factors which make ANN superior to keep the power grid stable regardless of what and which scenario possibly occurs:

- i. No requirement of a mathematical model for a network and lesser computational effort with less iteration.
- ii. Lead to improved performance when properly tuned.
- iii. Robust for online static security assessment.

3.2 ANN Data Preparations

Predefined data has been allocated for Malaysia power system and extracted to fit into the neural network environment. The input data consist of generators and solar active power (G_{supply} , P_{solar}) together with load active and reactive powers (P_{Load} , Q_{Load}). While the target outputs are the node voltage and load margin. At this point, node number 11 is determined as a weakest bus thus apparently being adopted to embrace for loading margin classification investigation. Theoretically, each ANN model consists several numbers of inputs that are linked to a summing junction. The inputs values are then multiplied by competent weights and aggregated with other inputs. The process of training that been injected into the model will change the values of weight connection and yielded the effect of changing input link's strengths. The value of aggregated and weighted inputs is deployed into activation function to be scaled in proper ranges towards output layers. There are several common activations or transfer functions available such as a tangent sigmoid, linear and log-sigmoid but in this study, a log-sigmoid activation function is utilized due to its positive returning integer as defined in Fig. 8 and Eq. (1) apparently. Furthermore, the framework model of input and output characteristics is illustrated in Fig. 3 which depicts typical neural network structure behaviour.

$$F(z) = \frac{1}{e^{-z} + 1} \quad (1)$$

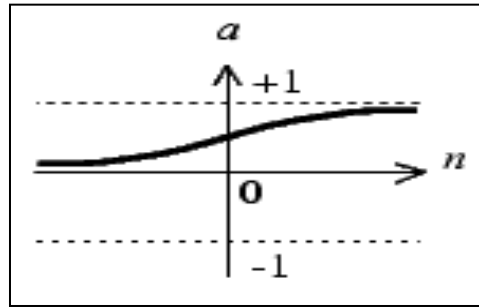


Fig. 3.1. Log-Sigmoid Activation Function

Aforementioned, few factors are attained to yield astral results from this ANN model, for instance, pertinent inputs were given, a number of hidden layers or neurons utilized and learning algorithm modification. In a class of static model, Radial Basis Function (RBF) supposed to have better performance compared to Multi-Layer Perceptron (MLP). Identically both methods are splendid if only they are deployed thoroughly to meet specifically given network system.

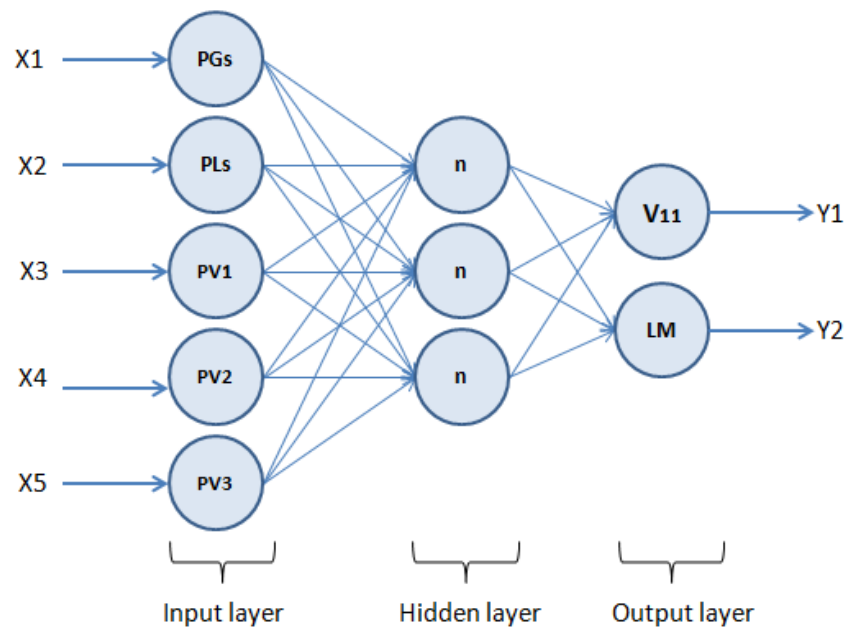


Fig. 3.2. Neural Network Structure Model

The attribute factors that mainly affect to ANN performance are its layer and neuron quantity inside the network hence a meticulous refinement has been done in this investigation for both approaches. Even though RBF is superior to MLP, vividly throughout this study MLP seems to be in favour oppositely and this is proven profoundly in the following constructive simulations.

In Fig. 10, Continuous Power Flow (CPF) has been used to calculate loading margin with having multiple of inputs which attained from the power utility. The set of simulation results by then were deployed into Artificial Neural Network via MLP and RBF model respectively to yield a further classification of loading margin.

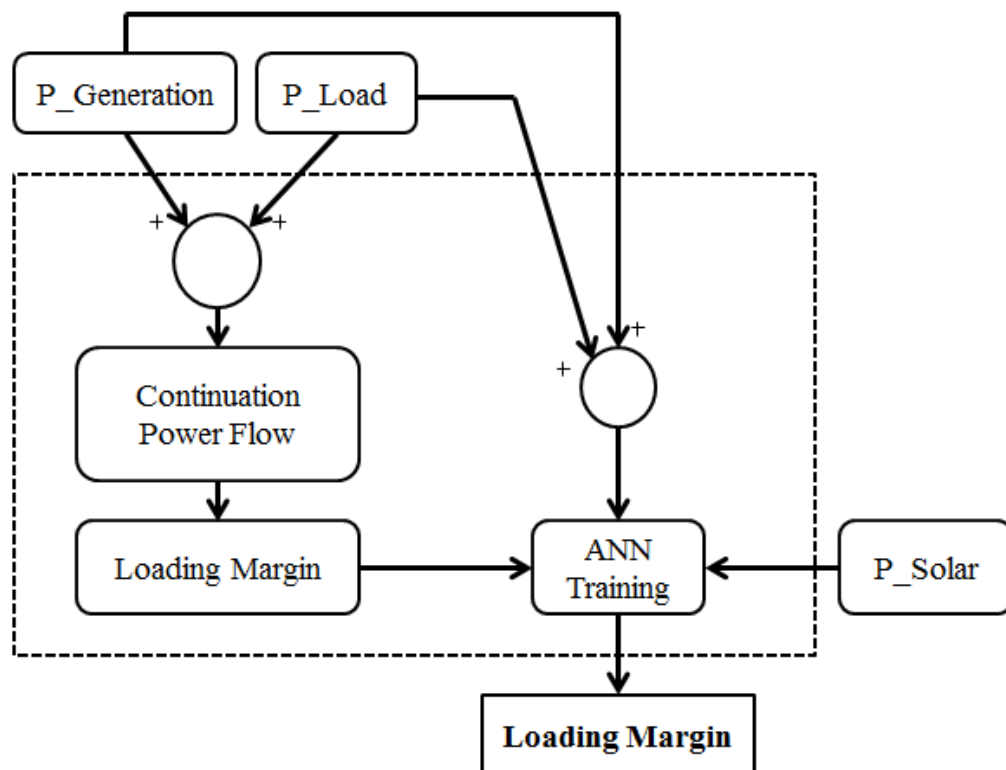


Fig. 3.3. Process of Computing Loading Margin

Particularly selection of parameters used has been chosen meticulously as shown in Table 2. As for MLP and RBF networks, the number of neurons in the hidden layers are fixed at 20 and 50 neurons because if too many neurons are deployed the training time may become excessively long or come to worse it would overfit the data. The overfitting problem will incur the network to model a random noise in the data resultants for unseen data to be generalized. So, there is no single formula for selecting the optimum number of hidden neurons that is it comes back to several occasions of experimentation until a reasonable number of neurons were determined and evaluated. In practice, to have one or two hidden layers are widely used which give good performances hence in this study only one hidden layer being utilized in which total three layers being adopted including input and output layers respectively. In a nutshell, the rule of selection for the network should be the one that performs the best in the testing set with the minimum number of hidden neurons and literally, all other parameters must be kept constant to not make complication and create different error surfaces in the developed network.

Table 3.1: ANN Parameters

Type of Network	Number of Layers	Number of Neurons
MLP	3	20
RBF	-	50

3.3 ANN Performance Criterion

For evaluating the accountability of testing data, a Root Mean Square Error (RMSE) is used that pertaining the desired network behaviour. This approach is a good measure for fitting purposes which allows for variation observations in the measurement of any typical point. The RMSE is being used to measure the difference between the predicted values and the actual values observed from the circumstances that are being modelled and further aggregate them into a single measure of predictive power. It can also be illustrated with a

graphical figure on measuring the effectiveness of fitting measurement between actual and estimated values.

$$\text{RMSE} = \sqrt{\frac{\sum_{i=1}^n (X_{\text{real},i} - X_{\text{target},i})^2}{n}} \quad (2)$$

Where N is the number of data P_f^i is the predicted value P_f^i is the actual value and i is the number of allocation period for predicting.

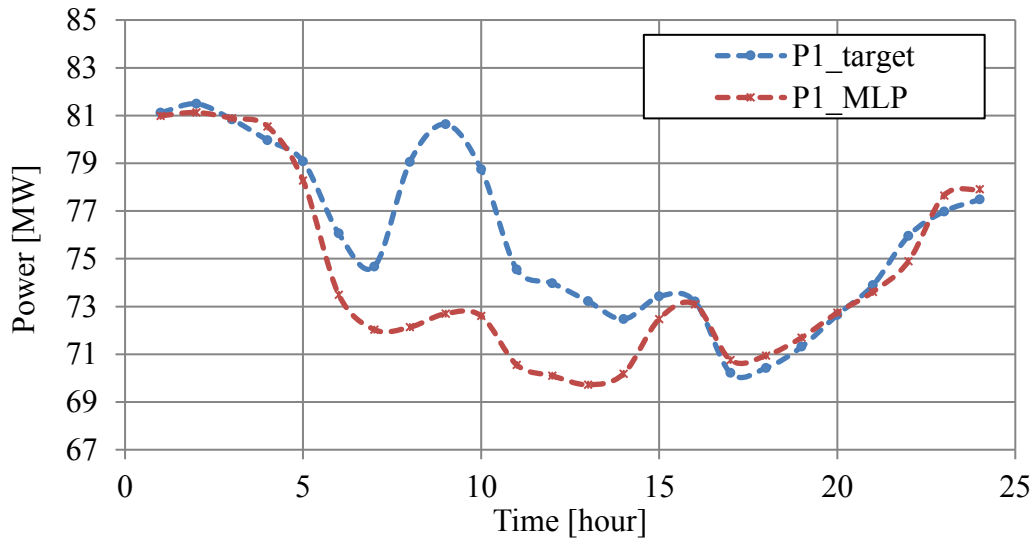


Fig. 3.4. Multi-Layer Perceptron Network Classification

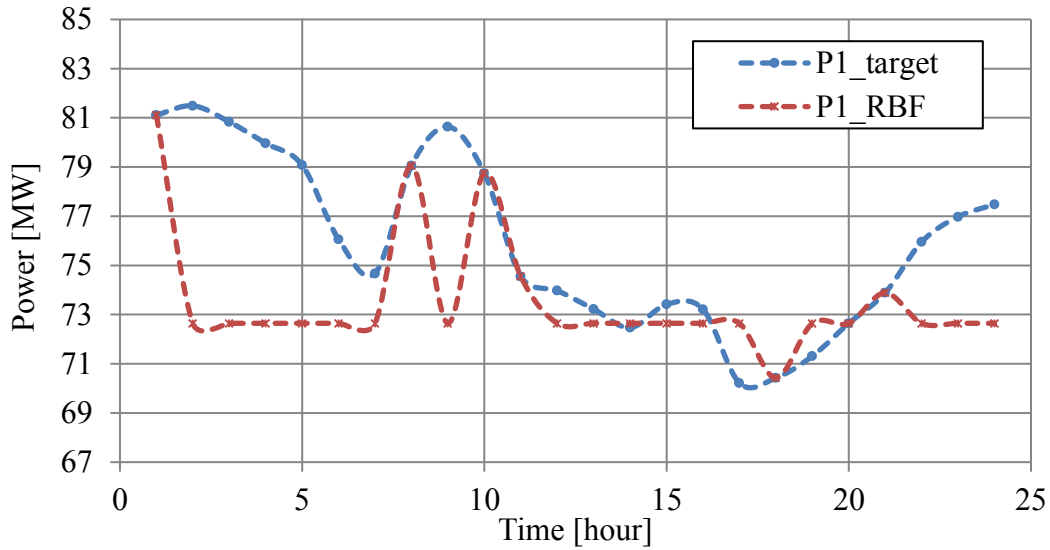


Fig. 3.5. Radial Basis Function Network Classification

The comparison between MLP and RBF network are presented in Fig. 11 and 12. These measurement has been tested with collective data from power utility in Malaysia and yields the results for loading margin estimation via both neural network approach as above and in Table 1. Seemly throughout this investigation, the RBF algorithm does not go well with the current test system whereby from training and testing process it shows that it could not satisfy and match few criteria acquired for instant active power output as illustrated in both figures and obviously MLP classification towards the estimation target is more refined compared to RBF classification. It shows a wild fluctuation with RBF environment seems counterintuitive in enumerating further investigation on attaining targeted outputs. The RBF training likelihood more susceptible to an error by then deteriorated the resultants at this point.

As comparison shows in Table 3 of CPF and ANN approach, it can be clearly seen that computation time taken for CPF is much longer in yielding intended output whilst ANN undoubtedly apprehended and reduced those figures by almost 50% at least with MLP network for instance. This kind of strategy is crucial for online power system operation and aided in ensuring any countermeasures deployed during fault by system operator is not violated or stumble at a certain level. Every second are counted and consider precious for

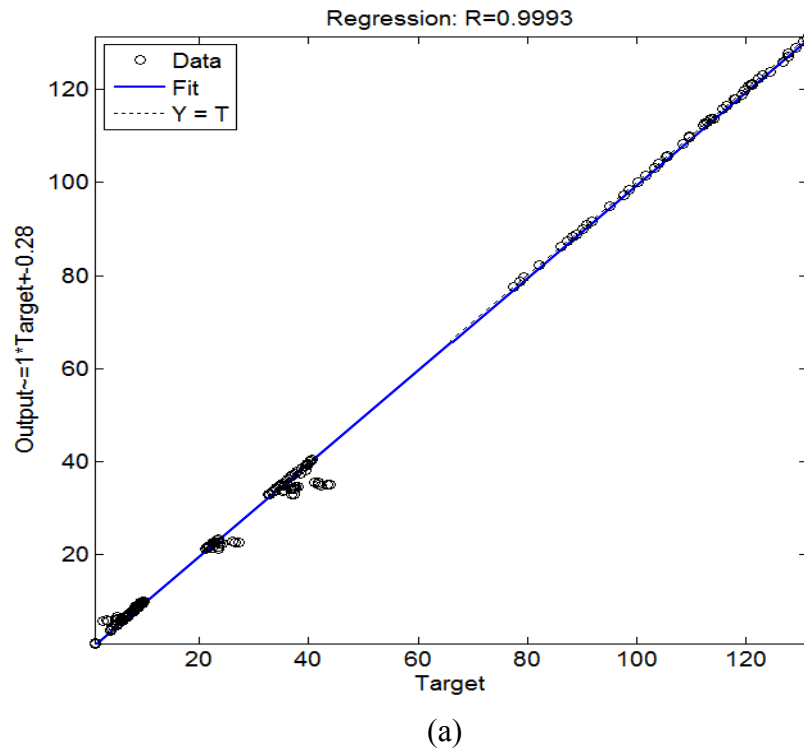
making not only right but also the justifiable decision in any practical online operation because any violation made could influence consequently to another party and resultants in a severe impact.

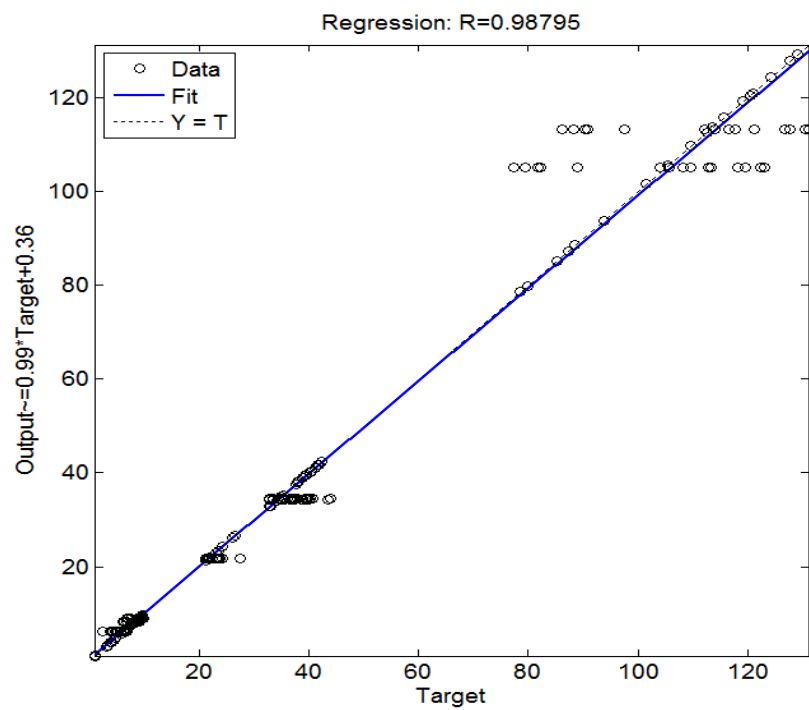
Table 3.2: Comparison between MLP and RBF Performances

	CPF	MLP	RBF
Time, sec	251.27	113	12
Iteration, steps	581	500	25
V_{\max} , p.u	0.6641	0.8952	0.991
Maximum Error	-	0.8338	9.2606
RMSE	-	2.048	2.3313
Spread	-	-	13

Furthermore, this observation can be detailed out by plotting the regression and calculating the error for both MLP and RBF which are $R=0.993$; $RMSE=2.0742$ and $R=0.98795$; $RMSE=3.1747$ respectively. Graphically, it is showed that RBF data of estimation a bit scatters away from the target line as shown in Fig. 13 (a) and (b). It has been tested that with quite a such number of errors in RBF training makes the estimation variables diverting away from the actual output been expected. Consequently, it can be said that the error should play a big role to get a substantial solution and this can be seen from Figure 14 (a) and (b) show by the blue line which is training MSE. Likely for RBF although iterations

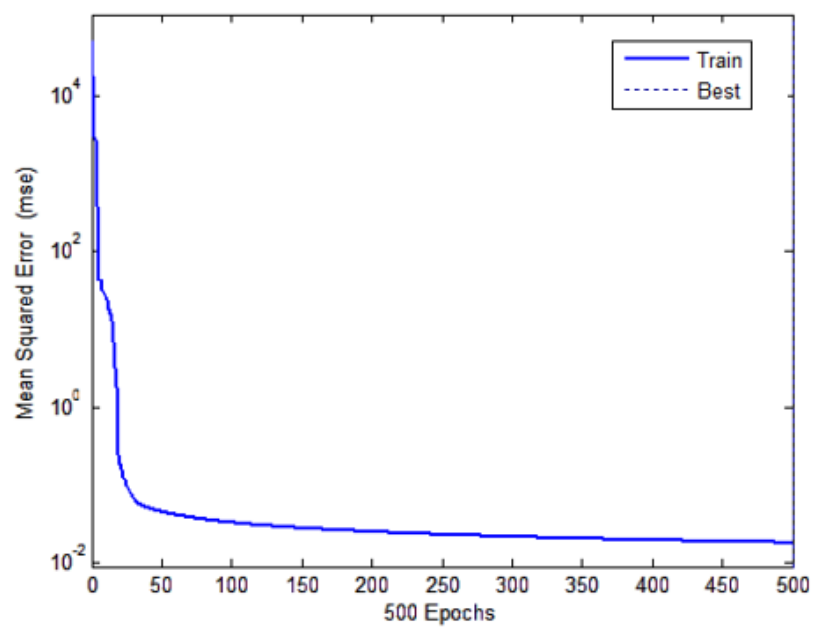
number is shorter but the elements slightly jumping around while for MLP the error convergence looks well trained and drop to small and stable value.





(b)

Fig. 3.6. (a) MLP (b) RBF Regression Plot



(a)

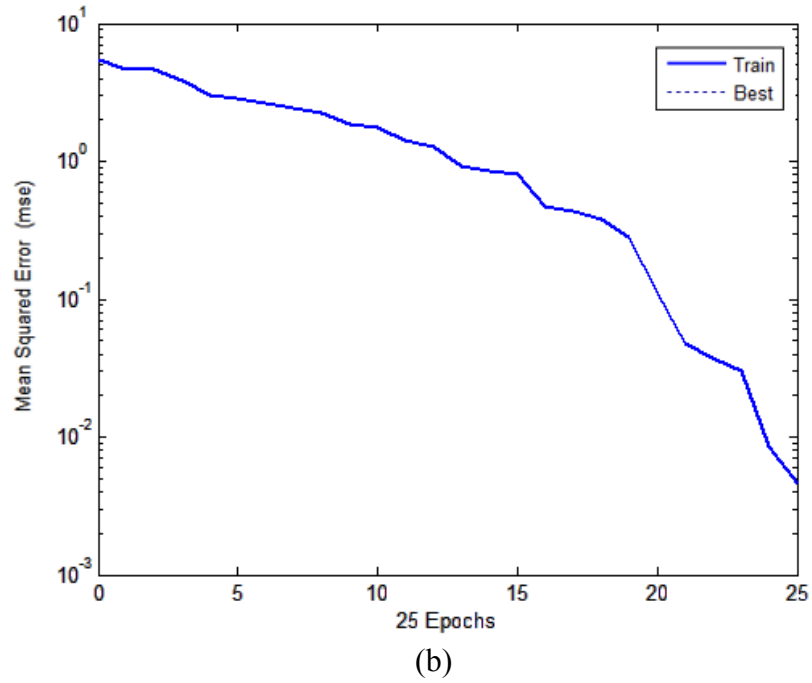


Fig. 3.7. (a) MLP (b) RBF Performance Plot of Error Convergence

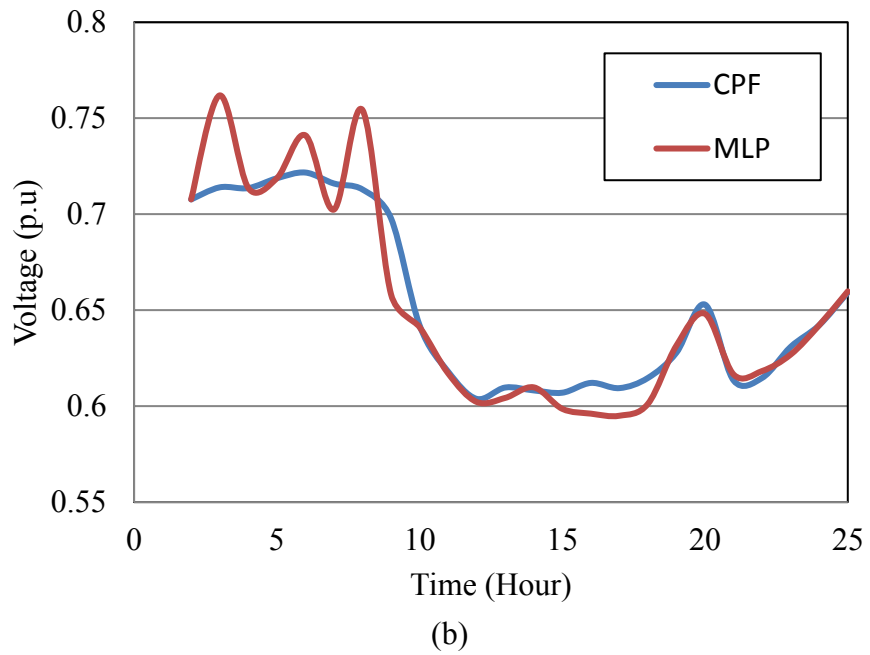


Fig. 3.8. Voltage Profile at Weakest Bus

To verify the proposed method, it has been tested daily operation for real network demand parameters. Basically, solar power variation is incorporated at several determined locations namely north, central and south area respectively. It must be acknowledged that solar power uncertainties are not treated deeply by any means using any kind of stochastic or probabilistic analysis but satisfactory with a variation of insolation for daily basis operation, thus presumably further delineation for substantial investigation could be content as well. In that meaning, ANN has been trained with an equivalently real collective set of variation data in advanced and hence successfully accommodated online operation employment with prior information indeed. Reliance on predictions of future solar energy input widely adopted by most energy sectors and power plant scheduling, power trading and grid operation are some examples by which can only be carried out optimally when reliable prediction are formed and available for the following hours and days, undoubtedly, with ANN alternatives.

Eventually, in the previous study had shown that central area was the strategic site for having more penetration of solar power thus for this investigation same approach is adopted. From Table 4, a decent and deterministic approach of loading margin estimation via MLP network is employed whilst decently compared with conventional CPF method for daily basis operation. Explicitly both methods show significant similarity which undisputedly denotes MLP method immensely embrace for loading margin verification.

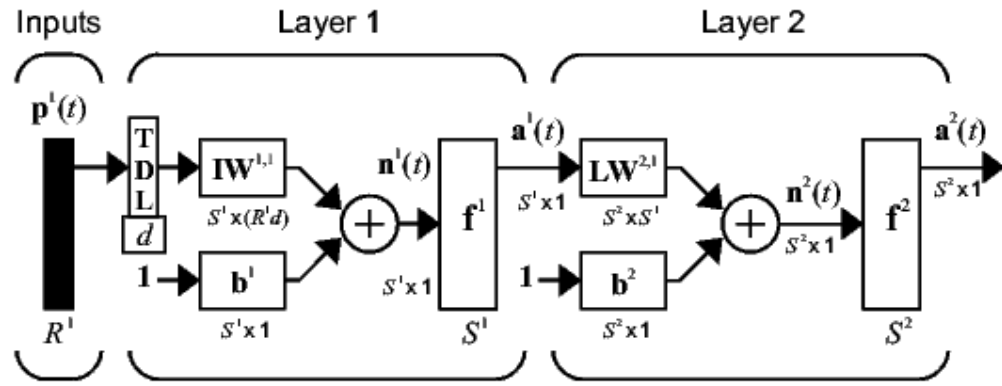
Table 3.3: Comparison between CPF and MLP Performances

Time (hour)	CPF	MLP	Deviation (%)
	LM (MW)	LM (MW)	
1	14.4609	14.46	0.001
2	13.5983	13.73	0.132
3	13.1411	13.14	0.001
4	12.8793	12.88	0.001
5	12.6282	12.69	0.062
6	13.0726	13.03	0.043
7	13.6964	13.82	0.124
8	15.5601	15.44	0.120
9	22.8378	22.86	0.022
10	27.1242	27.1	0.024
11	30.3352	30.47	0.135
12	29.8378	29.95	0.112
13	28.664	28.68	0.016
14	31.1211	31.34	0.219
15	31.6927	31.98	0.287
16	31.9406	32.27	0.329
17	30.5315	30.7	0.168
18	24.3572	24.37	0.013
19	21.9346	21.92	0.015
20	27.2412	27.22	0.021
21	26.8456	26.85	0.004
22	25.1857	25.19	0.004
23	22.7187	22.72	0.001
24	20.5741	20.57	0.004

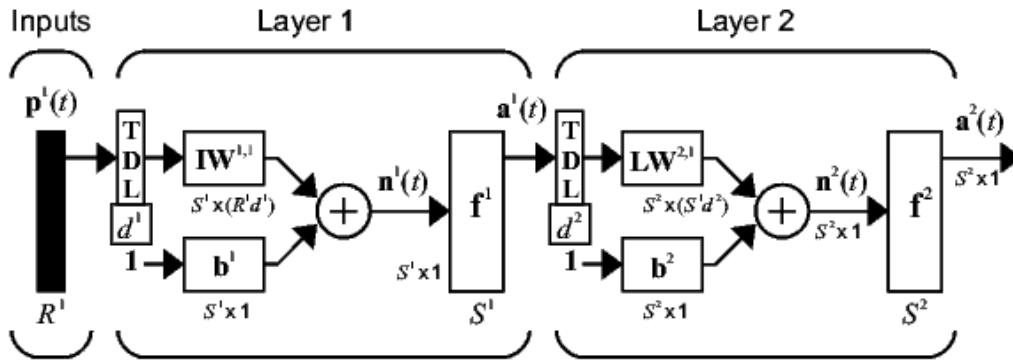
3.4 Focused Time Delay Network

The neural network itself is a static (linear or nonlinear) system, so it is only the input characteristic can be introduced the dynamics into any specific system. There is two kinds of the network in Artificial Neural Network (ANN) vicinity namely static and dynamic network. An ability to learn from previous data presented so called properties is a crux that draws a line between both networks. In a static network, the properties of a built model remain unchanged once been training but as for dynamic network it will try to adapt and keep learning during operation thus with this regard, it distinguished both performances indisputably.

To deal with the nonlinear multivariable pattern of time-dependent, a dynamic neural network is the best option, though. Comparatively, it differs from Multilayer Linear Neural Network (MLNN) which is a static model whereby Focused Time Delay Network (FTDN) has the ability to adopt a dynamic approach in its task. Time-delays in the dynamic neural network can either be distributed (DTDN) or focused (FTDN). The only different here is that in Distributed Time Delay Network (DTDN) the tapped delays lines are distributed throughout the network while in FTDN tapped delay line memory exist at inputs layer only as depicted in Fig. 16 (a) and (b). In addition, the weights of this kind of model are being shared among the neurons oppose as in the static model. It is presumed that the network currently operated one step ahead which considerably propounds a dynamic behaviour of time variant oriented. Moreover, the magnitude of the adaptation is controlled via learning parameter which decays over time hence execute faster than fully connected multilayer perceptron (MLP). To delineate dynamic model precisely, it consists two types which are those that have an only feed-forward connection and that have feedback connection. In this study, FTDN is considered because somewhat it does not need dynamic backpropagation for training purposes as in DTDN which consequently slowed down the iteration process.



(a)



(b)

Fig. 3.9. (a) FTDN (b) DTN Layout

3.4.1 Tapped Delay Line (TDL)

The tapped delay line represents the focused of input that stores the past samples of inputs. This process only occurs at the input layers, not throughout all hidden layers and output layers. That is why it is named after Focused Time Delay Network (FTDN) as the memories existence is only at input layers. Next, after updated iteration of the input is reached then the outputs from input layer are passed through the hidden layer and finally processed to approximate next expected a sample of output data. In this procedure, a number of neurons are set between $n=5$ and $n=20$. For normal case means excluding contingency only 5 neurons are utilized however as for line outage cases the neurons need to be increased to avoid divergence of data when training. More neurons mean more data been trained and eventually it will increase the time of iteration in fact sometimes the output yielded unnecessarily or indecently from the target.

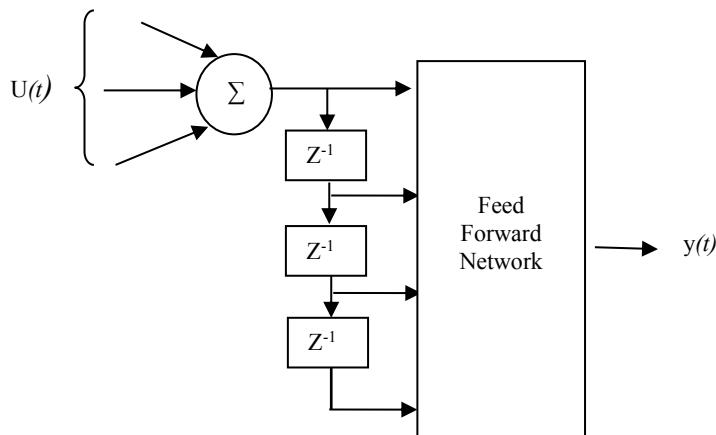


Fig. 3.10. Delay Line at Input Layer

The delay line is a kind of memory structure located only at input layers in FTDN which used along with static multilayer neural network. As shown in Fig. 17, the input signal enters from the left into the summing junction and passes through $N-1$ delays. Here, the tapped delay line sends to the weight matrix a current signal, previous signal and delayed signal. On top of that, the delays must appear in incremental order as well. The final output

is an N-dimensional vector based on the number of delays applied during training methodology for any network application. As such, to achieve a suitable dynamic approximation an appreciable number of delayed inputs may be enforced or prescribed, with an analogous significant in the number of network weights.

3.4.2 Inter-Regional Power Transfer in Malaysia Topology

The dynamic behaviour of demand power is treated using FTDN components to endeavour realistic output for permissible operation in MEPS network. Figure 4 represents the reflecting layout as shown previously in Fig. 18 for the interface flow between the regions in MEPS, which are simply divided into five regions. There are purposely divided into five regions due to geographic location, the density of population and distance. For example, Eastern region is situated far away from the Central region, experience uncertain weather and less demand capacity.

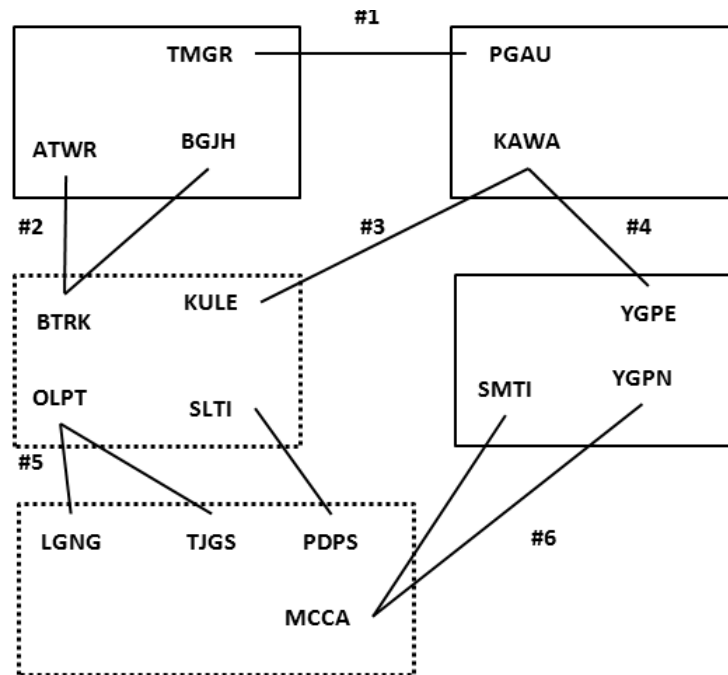


Fig. 3.11. Inter-Regional Route Linkage in Malaysia Power System

The Central and South-Central in this investigation are combined become a single region under a name of Central representing as a big metropolitan city. Furthermore, routes that connected among them are determined as depicted in Table 5 and the aim is to investigate a tie line flow between the Central region and the neighbouring regions denotes as route Number 2, Number 3 and Number 6 respectively. Central region undoubtedly compact not only with citizens but also commercial and office operations ongoing. These two industries concurrently attained higher demand at peak hours compared to residential per load curve observation. Contingency evaluation is the heart of system security assessment at all levels of the decision as if by neglecting it power system would run stochastically without proper protection planning and management provision. About this, a list of simulated contingency cases in MEPS network is simulated and presented with line outage for line Number 2, 3 and 6 correspondingly.

Table 3.4: Selected Line Outages

Line	Interfacing Line
Number #2	BGJH – BTRK ATWR - BTRK
Number #3	KAWA - KULE
Number #6	MCCA - SMTI MCCA - YGPN

It is presumed to get less than 10% deviation between training and testing readings and it yielded around 2% hereby conclude this model could satisfy for upcoming real-time operation not only for normal condition but also for contingencies events. The network might gain some insight in getting a kind of brisk information which utmost required for online operation and can encounter whatever and whenever uncommon things come into action.

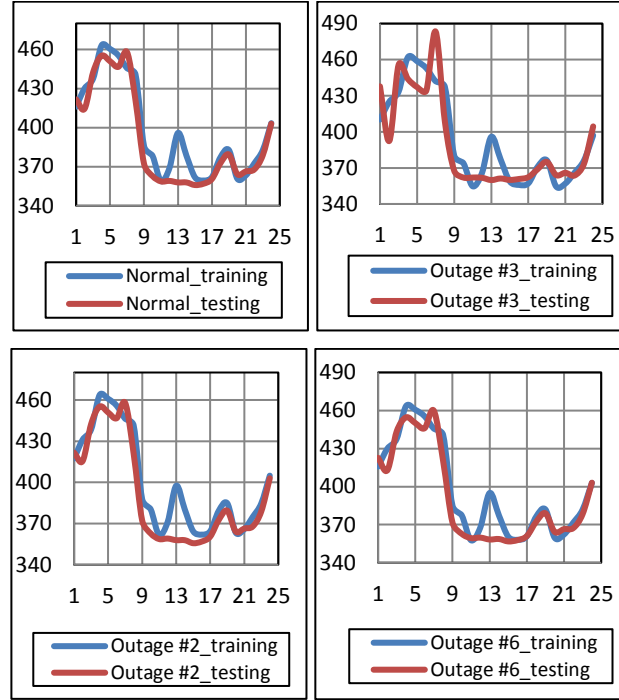


Fig. 3.12. Comparison on Interface Flow Margin for Daily Basis via Neural Network Training and Testing

3.5 Summary

The challenges brought by integrating ever more solar energy either at low or high-level voltages to achieve necessity target of national grid power system require transmission system operator devoted innovative mechanism across the power system security for voltage stability margin analysis. In this chapter, an ANN strategy has been employed as the machine learning approaches that capable of enumerating deliberately many input data in learning a nonlinear relationship between the operating states of the power system. This method has been successfully used to estimate the load margin quickly under normal and contingencies conditions by applying it to 275 kV Malaysia Power System model. It is the timely implementation of brisk online screening and accessible corrective offset concurrently that will let Malaysia Power System network continuously deliver effective and flexible

capacities in supply and demand balance scenario with the advent of solar provision for grid consumer's acceptability and resiliency aspects. The requirement of strenuous effort from operators will be ease in deciding and judging instant online action deterministically. Finally, this useful ANN concept utterly should not be limited for this purpose but could be extent for other implementations such as interface power flow and fault screening solutions profoundly with heuristic-based optimization mechanisms for instances.

CHAPTER 4

OPTIMIZATION FOR VOLTAGE STABILITY ENHANCEMENT

4.1 Introduction

Usually, network reinforcement is required when connecting PV plants with the network. However, it is possible to reduce the capital investment cost by the contribution of PV plants such as active power curtailment or reactive power support in order to mitigate the impact of their output. Hence, in this paper, the following scenario is considered.

- i. The optimal control method of PV plants under normal condition is proposed to improve the efficiency of power system operation.
- ii. Based on the above-proposed method, the optimal placement of PVs is determined from a viewpoint of the maximization of their contributions under normal condition.
- iii. With the given placement of PVs, another optimization method which maximizes LM under contingency condition is proposed to improve the voltage stability.

This section discusses the envisioned formulation of the above two optimizations. The first one is formulated as a constrained non-linear optimization problem to maximize operation efficiency considering voltage maintenance by using the active and reactive power of inverter-based DGs. In this formulation, the objective function consists of the following three terms: (i) minimize the transmission power losses in the entire network, (ii) minimize the voltage deviations at all the busses in the system, and (iii) minimize the total amount of

active power curtailment of all the inverter-based DGs.

Next, the second one is formulated as a maximization problem of LM in an emergency with fault occurrence under N-1 criterion. Generally, it is well known that the reactive power injection in demand side is effective to improve voltage stability by increasing system voltage. Here, it should be noted that active and reactive power outputs from DGs have a trade-off relationship under the current constraint of PCS. Namely, the active power curtailment is needed to increase reactive power if PCS capacity is not enough, in particular around peak time of active power output. Supposing reactive power of DG increases with active power curtailment, active power flow on transmission line has to be additionally increased by the amount of the active power curtailment in demand area although P-V curve can be enlarged by the reactive power support by DGs. This idea can graphically be illustrated in Fig.20 which indicates active power output from DG is now being curtailed whereas reactive power output is being increased so as to enhance LM. Moreover, it is supposed that the initial operating point (A) is now being shifted from its original position to the new one, (B), mainly due to the reactive power support from DGs. Now, original LM is given as $P_{C,A} - P_A$ meanwhile LM with DG control is given as $P_{C,B} - P_B$. Here, while the difference between $P_{C,B}$ and $P_{C,A}$ is regarded as the improvement of stability limit by reactive power support, the increased sending power, $P_B - P_A$, represents the decrease of LM inversely caused by this control.

Therefore, it is needed to determine the optimal balance of active and reactive power output which maximizes the LM by using optimization technique.

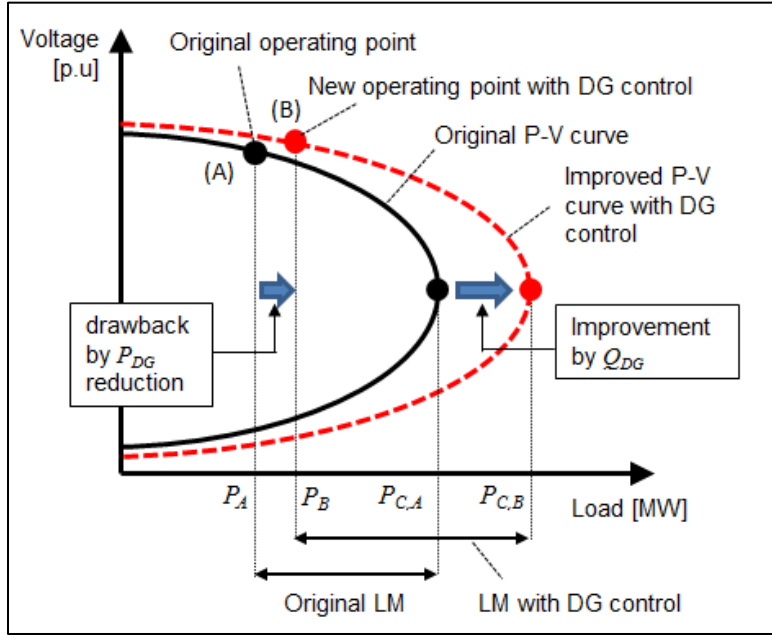


Fig. 4.1. Impact by PV Control on P-V Curve

4.2 Particle Swarm Optimization

Inspired by a social behaviour of fish schooling or bird flocking, thus a population-based stochastic and heuristic optimization technique of PSO as developed (56). PSO is employed by initializing a random solution of populations and searches for optima by updating generations. The main idea for this algorithm is a population called a swarm which generated randomly with the candidate solutions are known as particles by then moved around in the search space. The movements are at their random velocity guided with by their own best-known position and as they discovered new best position the process will be repeated until satisfactory solutions are obtained in finding values of the variables that minimize or maximize the objective function whilst obeying the constraints.

With an arbitrarily weighted acceleration at every time step, PSO will try to accelerate each particle towards its P_{best} and G_{best} locations as shown in Fig.21. In addition, the generic formulas for PSO algorithms are listed in Eq. (3), Eq. (4) and Eq. (5) respectively.

$$v_i^{k+1} = w \cdot v_i^k + c_1 \cdot r_1 (Pbest_i^k - S_i^k) - c_2 \cdot r_2 (Gbest^k - S_i^k) \quad (3)$$

$$w = w_{\max} - \frac{w_{\max} - w_{\min} \cdot x_{iter}}{iter_{\max}} \quad (4)$$

$$S_i^{k+1} = S_i^k + v_i^{k+1} \quad (5)$$

where,

w : the inertia weight

c_1, c_2 : acceleration constants

S_i^k : current position of agent i at iteration k

r_1, r_2 : two random numbers in the range of 0 and 1

$Pbest_i^k$: best position by a particle i at k^{th} iteration

$Gbest^k$: global best position in the entire swarm

The basic concept of PSO lies in accelerating each particle toward tentative best direction given by $Pbest$ and $Gbest$ with a random weighted acceleration at each time step.

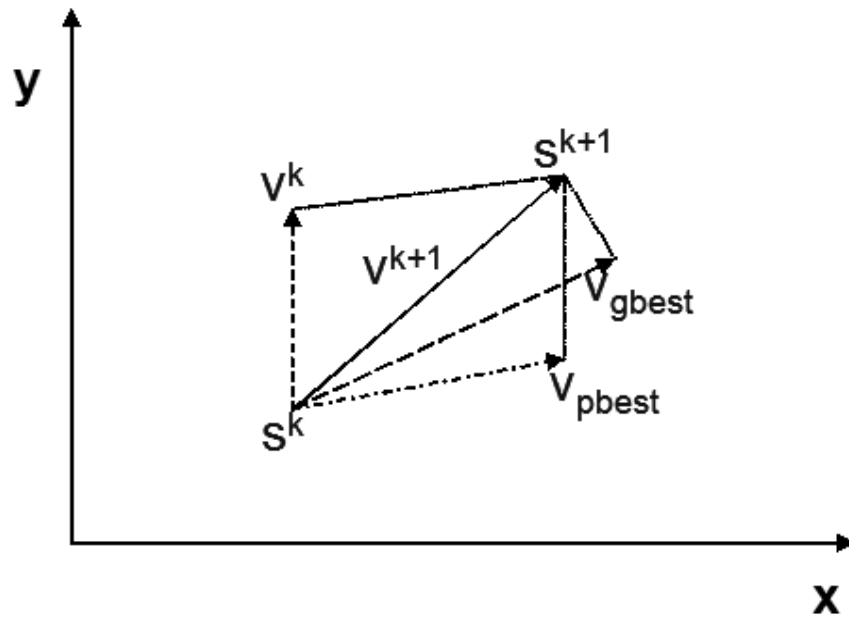


Fig. 4.2. Graphical Illustration of PSO Velocity Components

S^k : Current searching point

S^{k+1} : Modified searching point

V^k : Current velocity

V^{k+1} : Modified velocity

V_{pbest} : Velocity based on P_{best}

V_{gbest} : Velocity based on G_{best}

Understandably the implementation of PSO algorithm can be illustrated as a flowchart in Fig. 22.

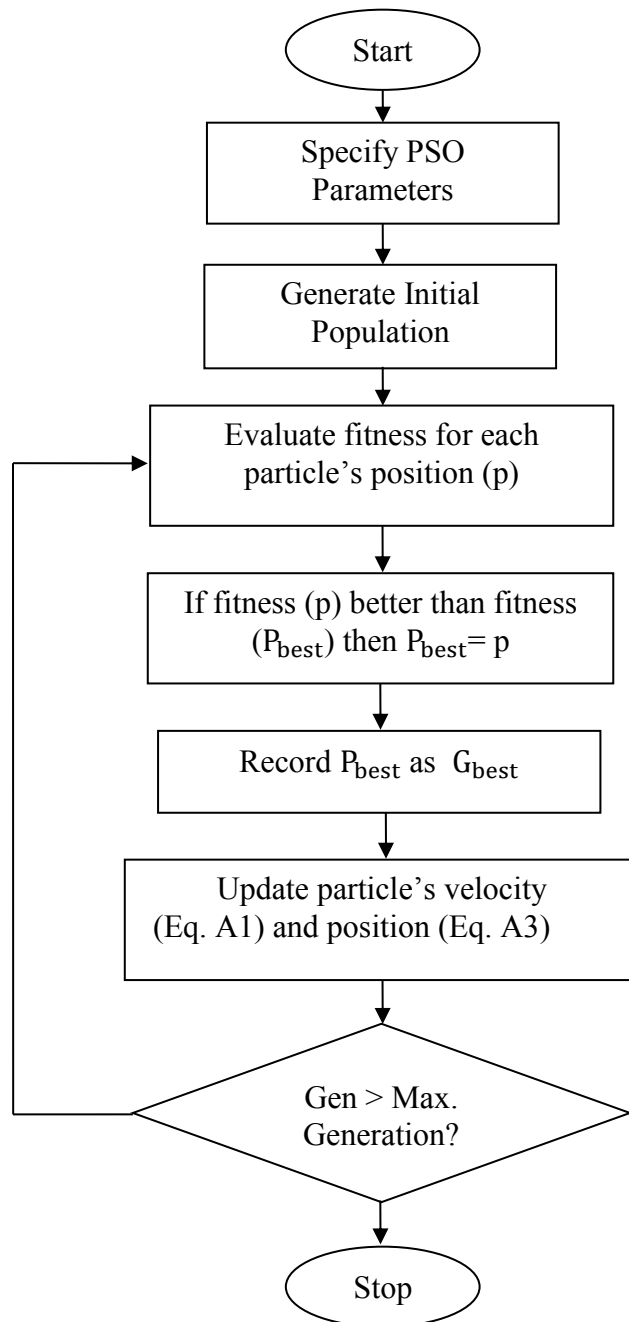


Fig. 4.3. Flowchart of the PSO

4.3 Continuous Power Flow (CPF)

CPF is used to trace the P-V curve given an initial point on the curve. By adding a continuation parameter or loading scalar, λ , the concept of predictor and corrector will be applied for the continuation process. By employing this CPF method, the steady state stability limit is determined to start from a known solution and estimated for subsequent solution correspondingly to a different value of load parameter. As for steady state loading limit, the basic power flow equations can be represented as:

$$g(x) = \begin{bmatrix} P(x) - P^{inj} \\ Q(x) - Q^{inj} \end{bmatrix} = 0 \quad (6)$$

$$f(x, \lambda) = g(x) - \lambda b = 0 \quad (7)$$

Where b is a vector of power transfer given by,

$$b = \begin{bmatrix} P_{target}^{inj} - P_{base}^{inj} \\ Q_{target}^{inj} - Q_{base}^{inj} \end{bmatrix} \quad (8)$$

Hence by composing b it delineates the effect of variation of loading or generation typically. In this investigation, a predictor and corrector method is implemented throughout the entire simulation. By having a better prediction, convergence process will be speeded up and tangent predictor estimation for the next solution is adopted as Eq.(B4).

$$z_j = [dx \quad d\lambda]_j^T \quad (9)$$

The tangent vector can be normalized and used to compute predicted approximation $(\hat{x}^{j+1}, \hat{\lambda}^{j+1})$ to the next solution.

$$\bar{z}_j = \frac{z_j}{\|z_j\|_2} \quad (10)$$

$$\begin{bmatrix} \hat{x}^{j+1} \\ \hat{\lambda}^{j+1} \end{bmatrix} = \begin{bmatrix} x^j \\ \lambda^j \end{bmatrix} + \sigma \bar{z}_j \quad (11)$$

Where σ is continuation step size parameter which affects the computational efficiency of the continuation method. Next, for corrector steps, the next solution (x^{j+1}, λ^{j+1}) is determined by correcting the previous predictor estimation and solve using Newton's method.

$$\begin{bmatrix} f(x, \lambda) \\ p^j(x, \lambda) \end{bmatrix} = 0 \quad (12)$$

The value of continuation parameter is parameterized to identify each solution so that upcoming solution or beforehand solution can be quantified as follow:

$$p^j(x, \lambda) = \lambda - \lambda^j - \sigma = 0 \quad (13)$$

4.4 Formulation for Normal Condition

The capability for reactive power support by DG basically depends on PCS capacity. The operating point in terms of active and reactive power has to be within the feasible region expressed as the inside of the circle as shown in Fig.23. Here, the circle, the boundary of the feasible region, represents the current limit of PCS. The maximum reactive power output depends on not only PCS capacity but also initial active power output (A). For example, reactive power control is available on the straight line between (B) and (C) without active power curtailment. The maximum reactive power output becomes larger as the original active power output decreases. If active power curtailment is allowed, it is possible to increase

reactive power output with reducing active power output from the original value. Namely, when reactive power injection is needed, the operating point can be moved from (A) to (D) at maximum through (C) with active power curtailment. In order to realize the contribution by DGs with reducing their active power output, the proper incentive should be given to the DG owners to compensate the loss opportunity cost caused by the curtailment. In this paper, it is assumed that the proper economic system was set out and active power curtailment with increasing reactive power output is available for the optimization.

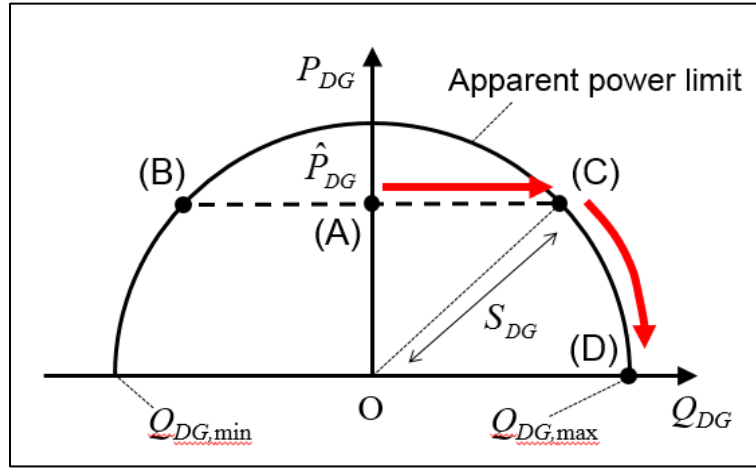


Fig. 4.4. Feasible Region of DG Control under Apparent Power Limit

Under the above assumption about the controllability of PCS, the optimization formulation for the normal condition is described as follows. First, based on the concept of multi-objective optimization, the objective function is given by f_1 as the following equation:

$$f_1(x) = \alpha P_{loss} + \beta V_{dev} + \gamma P_{curtail} \quad (14)$$

$$P_{loss} = \sum_{i=1}^{N_B} P_{loss,i} \quad (15)$$

$$V_{dev} = \sum_{i=1}^N \frac{\Delta V}{V_{i,ref}}, \Delta V = \begin{cases} V_i - V_{DBu,i} & \text{if } V_i > V_{DBu,i} \\ V_{DBl,i} - V_i & \text{if } V_i < V_{DBl,i} \\ 0 & V_i = V_{DB,i} \end{cases} \quad (16)$$

$$P_{curtail} = \sum_{i=1}^{N_{DG}} (\hat{P}_{DG_i} - P_{DG_i}) \quad (17)$$

where,

α, β, γ : weight coefficients of three objectives

N_B, N, N_{DG} : number of branches, buses, and DGs

$P_{loss,i}$: transmission power loss on branch i

$V_i, V_{i,ref}$: voltage and its reference value on bus i

$V_{DBu,i}, V_{DBl,i}$: upper and lower voltage of dead band on bus i

P_{DG_i} : active power of DG i

\hat{P}_{DG_i} : original active power of DG i without curtailment

P_{loss} , V_{dev} , and $P_{curtail}$ represent transmission power loss, the total amount of voltage deviation, and the amount of active power curtailment, respectively. It should be noted that dead band is set to the reference value regarding voltage deviation. Second, equality and inequality constraints are as follows:

$$P_{Gi} + P_{DG_i} - P_{Li} = \sum_{j=1}^N V_i V_j (G_{ij} \cos \phi_{ij} + B_{ij} \sin \phi_{ij}) \quad (18)$$

$$Q_{Gi} + Q_{DG_i} - Q_{Li} = \sum_{j=1}^N V_i V_j (G_{ij} \sin \phi_{ij} - B_{ij} \cos \phi_{ij}) \quad (19)$$

$$P_{Gi} = \frac{S_{Gi}}{\sum_{j=1}^{N_G} S_{Gj}} \cdot \sum_{j=1}^{N_G} P_{Gj} \quad (20)$$

$$\sum_{i=1}^{N_{DG}} P_{DG_i} + \sum_{i=1}^{N_G} P_{Gi} = \sum_{i=1}^{N_L} P_{Li} \quad (21)$$

$$P_{DG_i} = \begin{cases} \hat{P}_{DG_i} & \text{if } |Q_{DG_i}| \leq \sqrt{S_{DG_i}^2 - \hat{P}_{DG_i}^2} \\ \sqrt{S_{DG_i}^2 - Q_{DG_i}^2} & \text{otherwise} \end{cases} \quad (22)$$

$$Q_{DG_i, \min} \leq Q_{DG_i} \leq Q_{DG_i, \max} \quad (23)$$

$$V_{i, \min} \leq V_i \leq V_{i, \max} \quad (24)$$

where,

N_G, N_L : number of conventional generators and loads

P_{Gi}, Q_{Gi} : active and reactive power of conventional generator i

Q_{DG_i} : reactive power of DG i

G_{ij}, B_{ij} : conductance and susceptance of branch between bus i - j

ϕ_{ij} : displacement phase angle between bus i and j

P_{Li}, Q_{Li} : active and reactive power of load i

S_{Gi} : rated capacity of conventional generator i

S_{DG_i} : apparent power limit of PCS i

$Q_{DG_i, \min}, Q_{DG_i, \max}$: minimum and maximum reactive power output of DG i which are set as S_{DG_i} and $-S_{DG_i}$ in this paper

$V_{i, \min}, V_{i, \max}$: lower and upper limits of voltage on bus i

From above of Eq. (20) we would like to describe that it was supposed that generation dispatch is proportional to the generation capacity. Weight coefficients in the objective function reflect the relative importance of each single objective with respect to another. Although they should satisfy and follow transmission operator's planning and guideline accordingly, it is not so easy to determine them adequately from an academic point of view

but here, presumably $\alpha + \beta + \gamma = 1.0$. Therefore, in this paper, they are adjusted and normalized arbitrarily as $\alpha=0.2$, $\beta=0.3$ and $\gamma=0.5$, respectively.

4.5 Formulation for Contingency Condition

Generally speaking, when any contingency such as short circuit fault occurs, LM is largely decreased, in particular, as for loads which are close to the fault location. To avoid voltage instability phenomenon, the optimal active and reactive power output from DGs can be obtained by the following optimization formulation. The objective function is represented as Eq. (25) to maximize LM which can be calculated by Continuous Power Flow (CPF).

$$f_2(x) = \max LM \quad (25)$$

where,

LM : LM under uniform or single load increase

In solving CPF, there are two ways of increasing loads. One is to increase all the loads uniformly, and the other is to increase the only single load. In this paper, both of these two approaches will be used in the simulation as described in section 4. It is supposed that active power outputs of conventional generators are uniformly increased in proportional to their capacity to satisfy supply and demand balance. Here, all the terminal buses of conventional generators are firstly set to P-V specified buses. However, it should be carefully considered that reactive power output from conventional generators is available under various limitations such as armature current limit, field current limit, and end region heating limit (57). In this study, the feasible region of the conventional generator is modeled as a circle whose radius is its rated capacity for simplicity. When reactive power output reaches the maximum value to keep terminal voltage, the bus is changed to P-Q specified bus.

This paper deals with a rated capacity of DG's inverter regardless of other compensation devices such as load tap changer or switching capacitors because the main purpose now is to evaluate the contribution of DGs on voltage stability. As above, CPF can be solved under the same equality and inequality constraints as those for normal condition, from Eq. (18) to Eq. (24) with the following new one:

$$-\sqrt{S_{Gi}^2 - P_{Gi}^2} \leq Q_{Gi} \leq \sqrt{S_{Gi}^2 - P_{Gi}^2} \quad (26)$$

This equation was not considered in the optimization for normal condition supposing it was possible to keep terminal voltage to specified value without violating this constraint. Mainly PSO optimization is utilized in this investigation due to its reputation towards global utilization over cross engineering fields, efficient computation and slightly superior in average as opposed to other methods. Furthermore, as compared to conventional gradient-based optimization, we can deduce that PSO likely the best alternative to solve real and practical power system problems not only present but also in near future for congested power network typically. Previous authors (58) and (59) also had regarded the PSO as promising algorithm and outperformed others when applied to various problems for instances less susceptible to get trapped in local minima and more flexible as it used probabilistic transition rules. Moreover, from the beginning it is known that all the deterministic variables are continuous this time so, PSO is one of the best candidates for this study. Detailed descriptions CPF algorithms are presented as in Appendix A.

4.6 Supervisory Control Management

The desired active and reactive power from DGs can be determined through the optimization techniques for both normal and contingency conditions. However, in order to accurately obtain the optimized solution, full information of entire network has to be collected. As for the operation under normal condition, SCADA has been widely used for

monitoring the system state, and the obtained information here can be useful for the proposed method in this paper. However, regarding the contingency condition, it is strongly required that the optimal solution, which is in general different from that in normal condition, has to be determined in very short time after the fault occurrence in order to avoid the voltage collapse phenomenon. Since time cycle of data acquisition in SCADA is generally longer than this problem, it is impossible to obtain the optimal solution after the fault occurrence. Although applications of WAMS have been developed and actually used these days, the computation time should be another problem.

Therefore, the practical way is to obtain the optimal solution in advance as off-line calculation supposing the most serious fault occurs with the concept of N-1 criterion. The obtained optimal solutions are sent to all the PV plants at regular intervals. Each PV plant can change its operating point from optimal one for the normal condition to predefined new one for contingency condition when detecting the fault occurrence by observing the serious voltage drop at the terminal bus at its point of common coupling. This idea enables each PV plant to start the emergency control earlier without receiving the control signal from TSO, which can be regarded as decentralized control. Of course, the direct control signal is also effective if high-speed communication is available.

In the case of the above-decentralized control, it becomes another problem that accurate fault point is not known. When the actual fault point is different from that used in the optimization, the effectiveness of the predefined operating point is relatively lower. In particular, there is a possibility that LM is inversely reduced by the proposed method. However, by the proposed method, because the combination of reactive power injection and active power curtailment to some extent is usually obtained as an optimal solution, it is expected that the effectiveness of the proposed method is not largely decreased due to the assumption error. Therefore, in this paper, optimization for contingency condition is calculated only with the most critical fault case and obtained an optimal solution is used for all the fault cases.

Another issue is a possibility of over voltage caused by too much reactive power injection from PV plants. The optimal solution represents the best combination of active and reactive power from PV plants in order to maximize LM, namely, only very heavy power flow condition is considered. However, in the actual power system operation after the disturbance, over voltage problem can be caused by the same optimal output if load level does not change as shown in Fig.24 (operating point (B)). To cope with this problem, PV output can be adjusted not to cause the over voltage in a decentralized manner. Specifically, the reactive power output should be controlled by PI logic and its reference value can be given as optimal reactive power. Here, the control is deactivated when the terminal voltage of PV plant reaches the upper limit. As a result, the terminal voltage of PV plant should be firstly increased from operating point (A) to (C) in Fig.24, and then, it moves rightward as load increases. The operating point reaches the optimal solution at operating point (D), and the same optimal solution is kept even with a further increase of load in this figure.

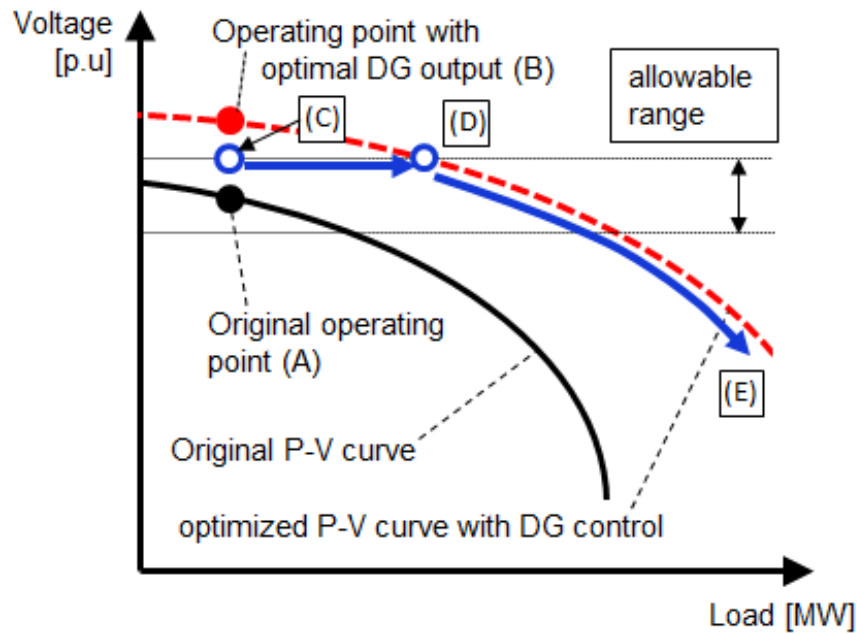


Fig. 4.5. Diagram of TSO Control Scheme for Contingency

4.7 Summary

This chapter presents the application of PSO and CPF for voltage stability study related to reactive power control with respect to load margin enhancement. It has covered the impact of solar PV participation with optimal operating points considering a number of constraints. Namely steady state and contingency scenarios are applied in this investigation and developed in the MATLAB environment.

CHAPTER 5

RESULTS AND DISCUSSION

5.1 Test System

Simulations were carried out by using Malaysian Electric Power System (MEPS) model with 7 generators and 9 uniform constant power loads as shown in Fig. 25. The impedance of transmission lines are shown in Appendix C. The minimum and maximum voltage limits are set to 0.9p.u and 1.05p.u, respectively. It is planned that solar power integration is highly progressed in the near future⁽⁶⁰⁾ in MEPS. Then, the PV is modeled based on the following assumptions:

- The total amount of PVs was set to 40% of the peak demand, namely, 6.6GW in the MEPS model.
- Insolation conditions are entirely the same within the MEPS, and locations of PVs can be arbitrarily planned.
- 6.6GW of PVs can be divided into three plants with the capacity of 2.2GW. Their optimal locations can be determined considering the impact on the network management as described in section 2.

Two optimization problems corresponding to normal and contingency conditions described in section 2 are tested in this section. In Table 6, the parameter setting for PSO algorithm used in this section is presented.

Table 5.1: PSO Parameters

Population	50
Maximum Iteration	300
c_1 and c_2	2
w_{\max}	0.9
w_{\min}	0.4

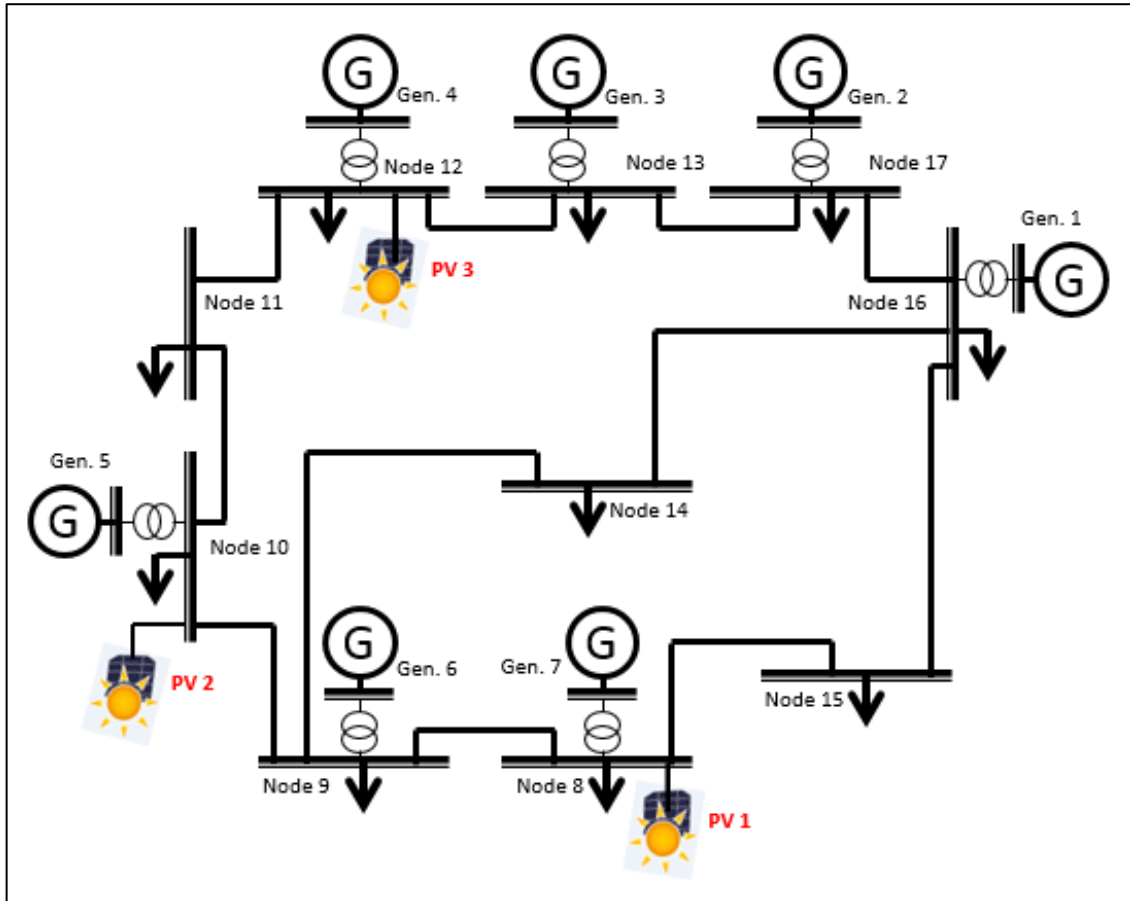


Fig. 5.1. MEPS Network Model

5.2 Normal Condition

In order to evaluate the PV's contribution to daily operation, the typical daily load curve, and insolation change are given as shown in Fig. 26 and 27. The overall PV generation

power is represented as GW, and the peak value of the generation output is corresponding to the rated PV output, 2.2GW at 12:30. The proposed method for the normal condition was repeatedly applied for all the installation patterns of three PV plants. As a result, bus 8, 10 and 12 were chosen as the optimal placement. This placement was also shown in the previous Fig.25. The optimized PV control in terms of active and reactive power output throughout a day is shown in Fig.28 and 29. In the morning and evening when the active power output of PV is small, reactive power output is used to reduce transmission power loss by improving the apparent power factor of loads.

However, as PV output increases, this reactive power output for power factor improvement decreases inversely because of the decrease of the free capacity for reactive power. However, the transmission power loss is still reduced also during the daytime because of the reduction of active power flow sent from conventional generators to loads. As a result, the transmission power loss minimization is achieved throughout the day as shown in Fig.30. In addition, by taking one time zone as an example, 12:30, it is shown in Table 7 that trade-off relationship between active and reactive power output under the constraint of PCS capacity was properly maintained because P_{PV} and Q_{PV} satisfy Eq. (9). Here, voltage profile is also controlled within the allowable range as shown in Fig.31. In this figure, the voltage profile without the proposed method is also shown at unity power factor. As shown in these results, the voltage deviation from the reference value (1.0p.u) was slightly increased to reduce transmission power loss although the voltage profile was originally within the allowable range.

Finally, it should be noted that various load curves and insolation patterns have to be considered stochastically based on the extraordinarily large amount of past data to achieve the practical optimization. However, in this paper, this issue is simply modeled because the most important aim of this paper is the contribution to voltage stability improvement to be described in the following section.

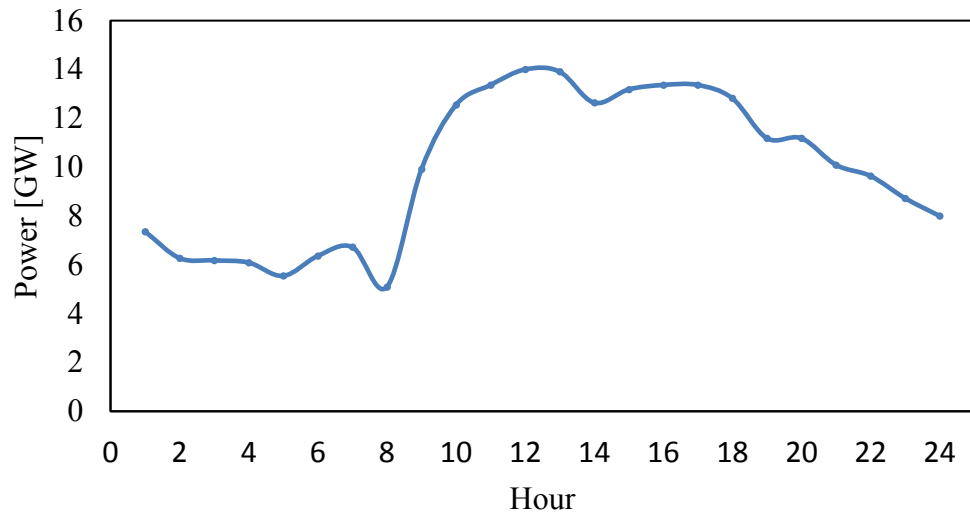


Fig. 5.2. MEPS Load Curve ⁽⁶¹⁾

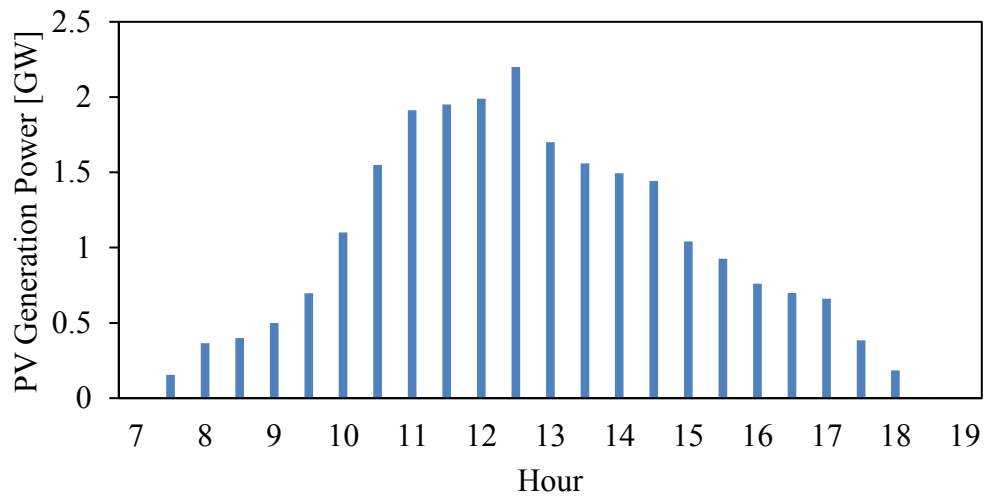


Fig. 5.3. MEPS Overall PV Generation Pattern

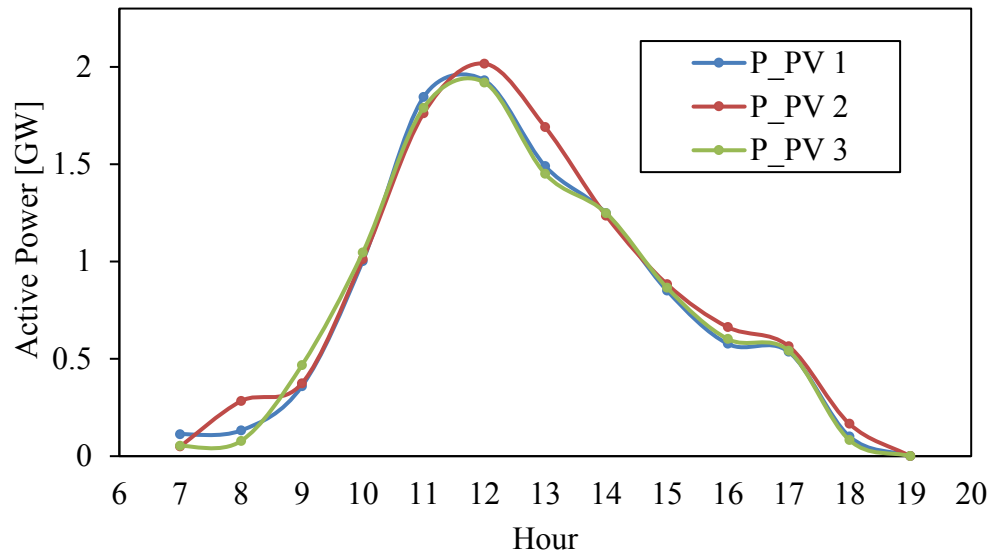


Fig. 5.4. Active Power Output of PVs via Proposed Method

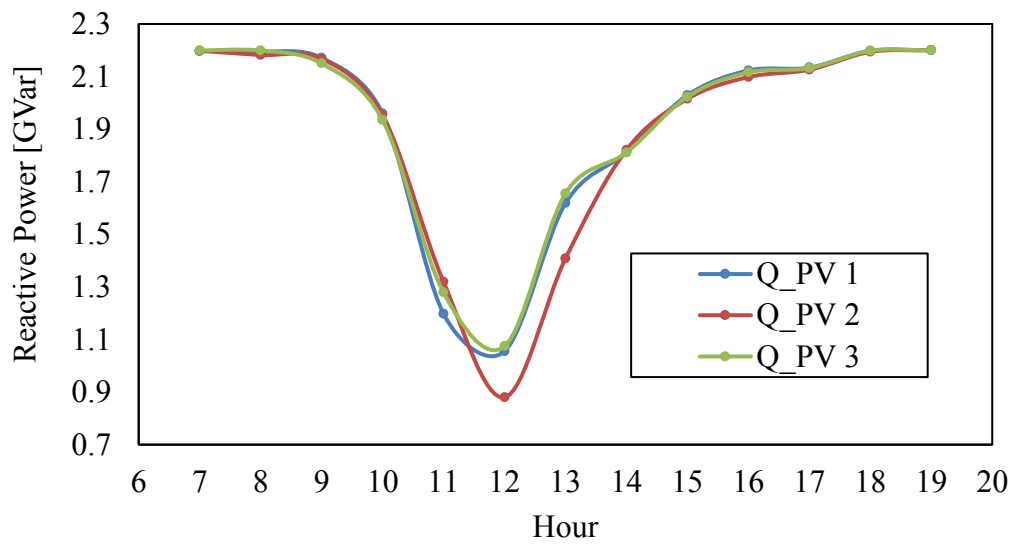


Fig. 5.5. Reactive Power Output of PVs via Proposed Method

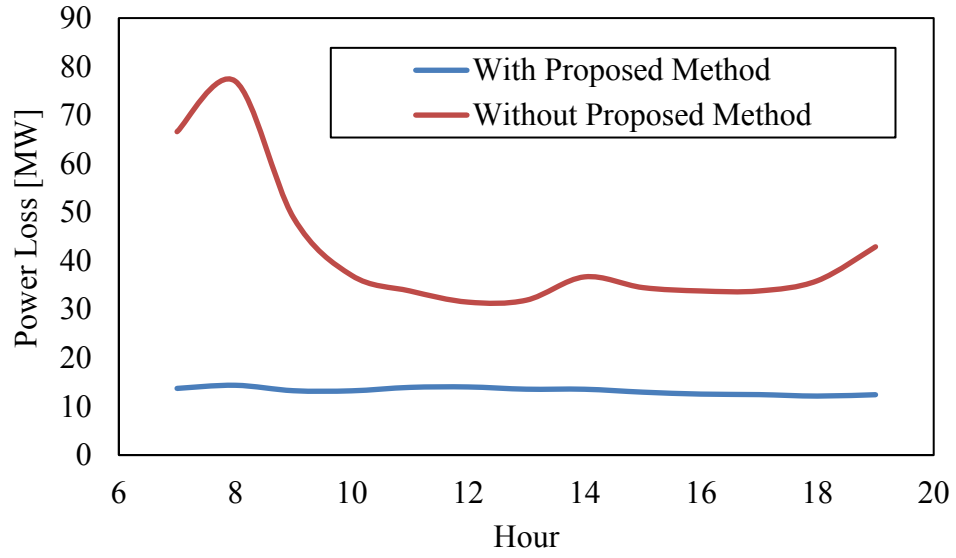


Fig. 5.6. Transmission Power Loss

Table 5.2: Optimal Solution for Normal Condition at 12:30

	PV 1	PV 2	PV 3
Bus Location	8	10	12
Active Power, P_{PV} [GW]	1.931	2.017	1.920
Reactive Power, Q_{PV} [GVar]	1.055	0.880	1.074

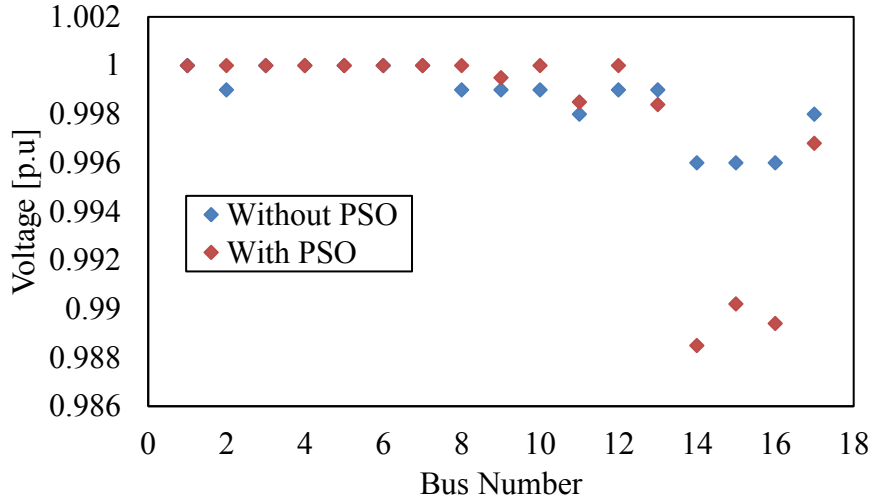


Fig. 5.7. Voltage Profile in Normal Condition at 12:30

5.3 Contingency Condition

In this section, the proposed method for LM maximization is tested based on maximum PV output and different two load levels, at 10:00 and 12:30, in order to show the proposed method works well under the load fluctuation. The locations of PVs are set to bus 8, 10, and 12 which are treated as the optimal positions in terms of operation under normal condition as described in the previous subsection. The proposed method was applied supposing transmission route 14-16 tripped due to the three-phase to ground fault as the worst case. Table 8 and Fig. 32 show the generation dispatch, loads, and power flow on transmission lines, at the both two cases. Here, bus 1 was treated as swing bus whose capacity is relatively larger than others, namely, the reactive power limit of this generator was not considered. Moreover, all the loads are uniformly 1181 [MW], 886 [MVar] at 10:00, and 1400 [MW], 1050 [MVar] at 12:30, respectively. Due to this fault, the power flow on “16-17” and “15-16” are largely increased. As a result, this fault gives a big impact on voltage stability, and this was the reason why this fault point was chosen as the critical fault point.

As described previously, there are two approaches to evaluate LM, which are defined as case 1 and 2, as follows:

Case 1: LM was evaluated with increasing all loads uniformly.

Case 2: LM was evaluated with increasing focused single load without increasing the other loads.

In plotting the P-V curve in next subsection, loading parameter, defined as the percentage of additionally increased load over the original load, is used in above each case.

Table 5.3: Generation Capacity and Dispatch

Gen.	Capacity [MW]	Generation Output [MW]	
		10:00	12:30
2	400	110.8	146.8
3	600	166.2	220.2
4	5373	1489	1971
5	911.1	252.5	334.4
6	9096	2616	3465
7	3200	1052	1173

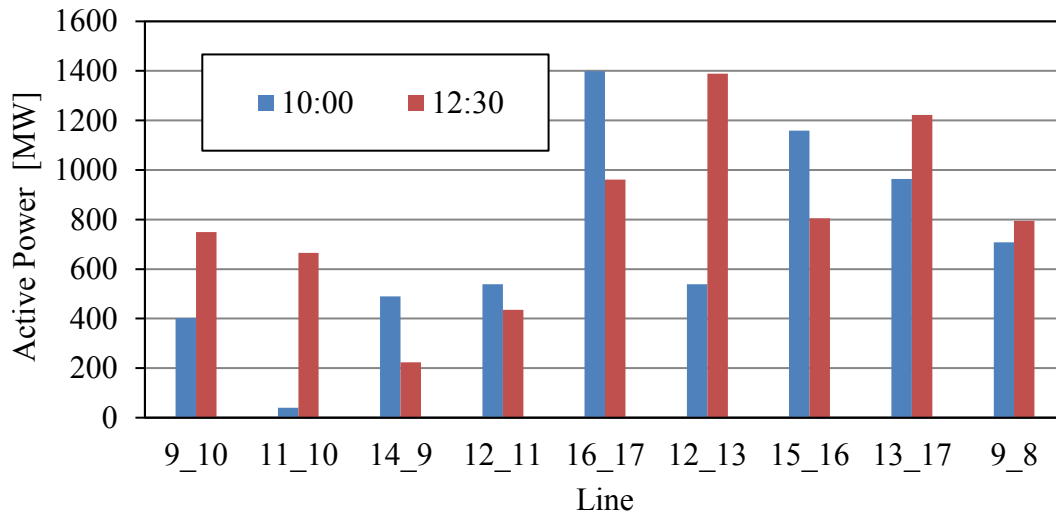


Fig. 5.8. Power Flow on Transmission Lines

5.3.1 Case 1 – Uniform Load Increase

A) Case 1 with light load

The proposed method was applied based on the Case 1 with a light load at 10:00. Fig.33 and 34 show P-V curves with and without the participation of PVs on bus 15 and 16 which are critical bus and its adjacent bus, respectively. It has been pre-determined for any bus that shows the smallest LM after contingency event will be chosen as a weakest bus which delineate for further support eventually. It is shown that P-V curves are enlarged by the proposed method effectively and loading parameter was increased by approximately 41.42%. Here, the trade-off relationship between active power curtailment and the reactive power increase is also considered. In addition, Fig.35 shows the voltage profile with the maximum loading at the stability limit. The voltage profile is almost the same with and without the proposed method. Although the voltage on top of the P-V curve is often increased by reactive power support at load side, this effect should be cancelled because of the voltage drop caused by the active power curtailment of PVs.

An optimized solution of the active and reactive power of PVs, in this case, is shown in Table 9. All the operating points are on the edge of the feasible region because the increases of both active and reactive power contribute to the LM maximization.

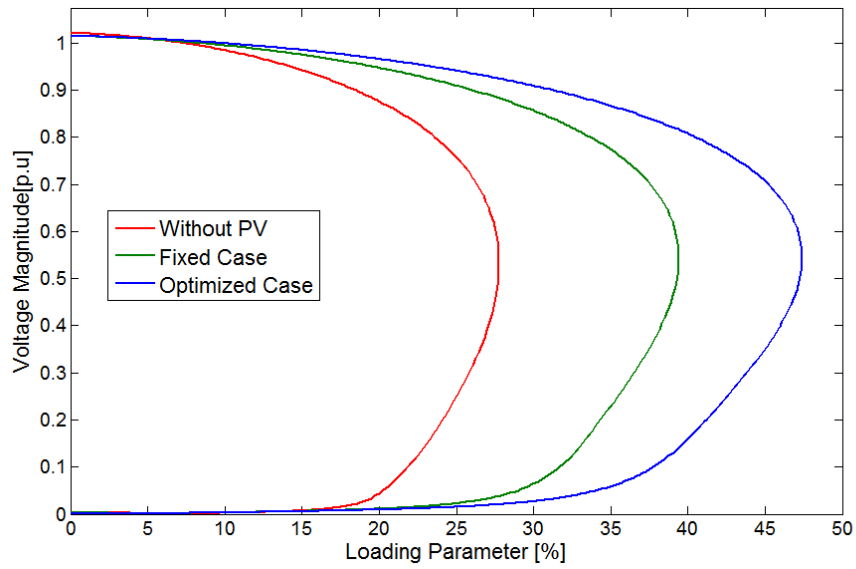


Fig. 5.9. P-V Curve at Bus 15 (Case1 with Light Load)

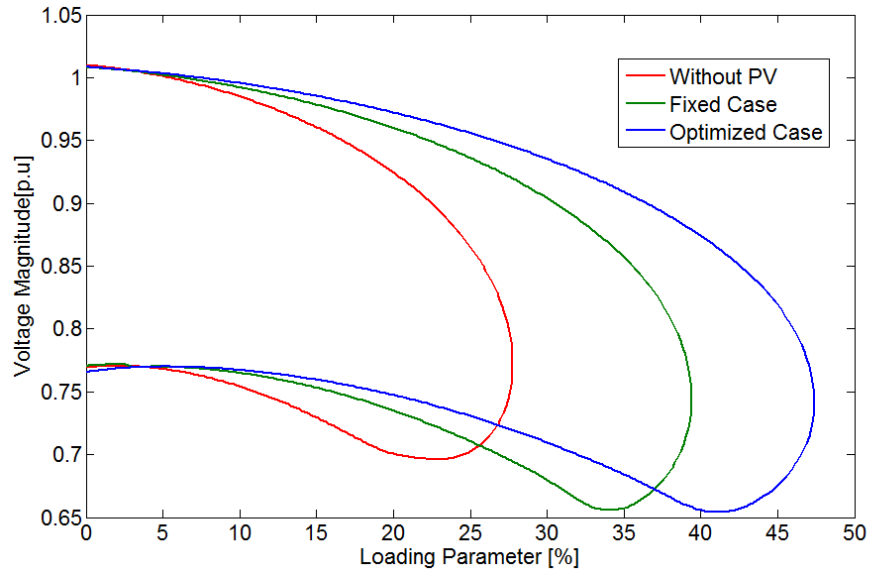


Fig. 5.10. P-V Curve at Bus 16 (Case1 with Light Load)

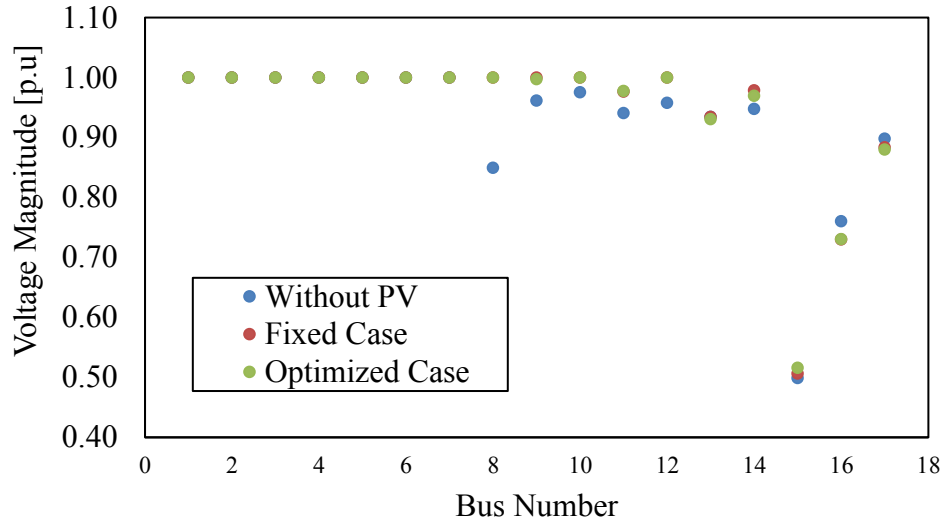


Fig. 5.11. Voltage Profile at Stability Limit (Case1 with Light Load)

Table 5.4: Optimal Solution in Case1 with Light Load

	PV 1	PV 2	PV 3
Bus Location	8	10	12
Active Power, P_{PV} [GW]	2.023	1.878	2.004
Reactive Power, Q_{PV} [GVar]	0.865	1.146	0.907

B) Case 1 with heavy load

The simulation results in Case1 with heavy load are shown from Fig.36 to 38, and Table 10. Compared to the light load case, the effect in LM maximization was slightly larger while the optimal reactive power of PVs was larger, in particular, at bus 8. Which means the voltage drop was larger with a heavy load and reactive power support should be essential to keep the system stability.

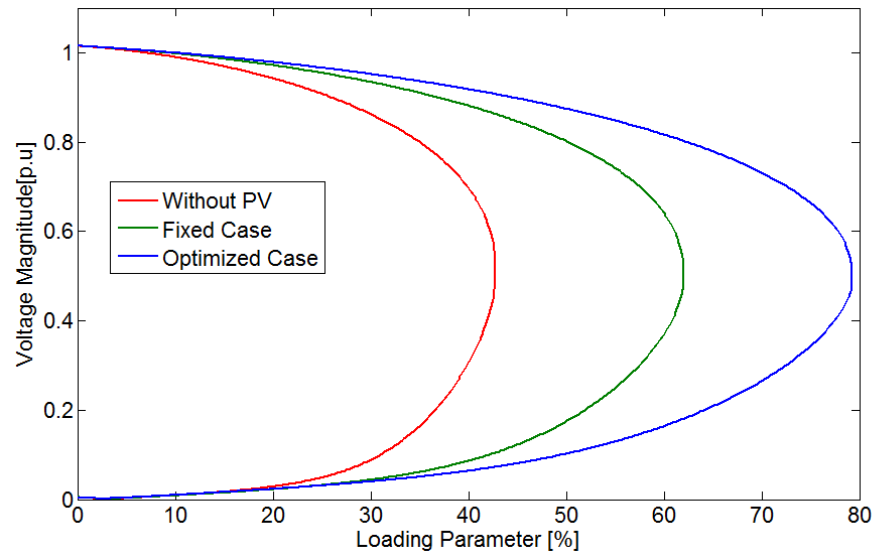


Fig. 5.12. P-V Curve at Bus 15 (Case1 with Heavy Load)

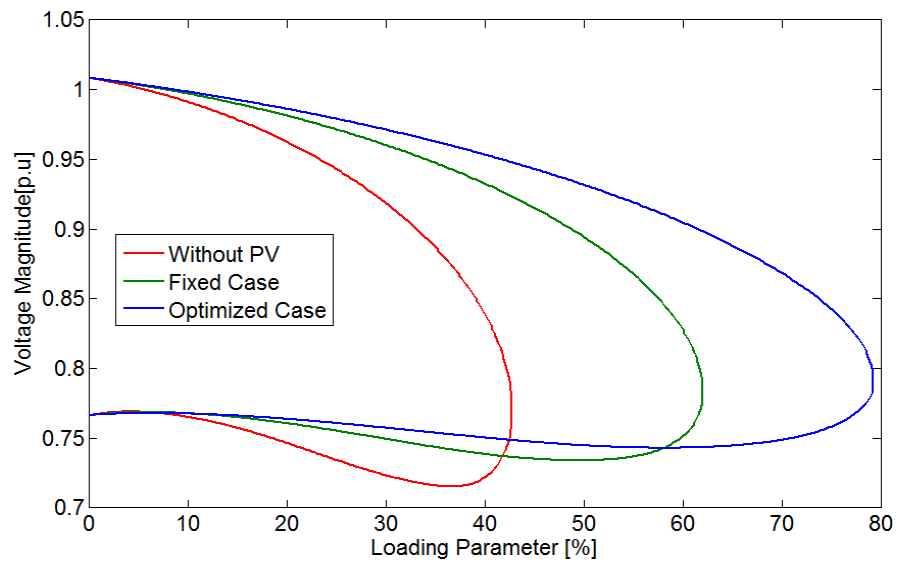


Fig. 5.13. P-V Curve at Bus 16 (Case1 with Heavy Load)

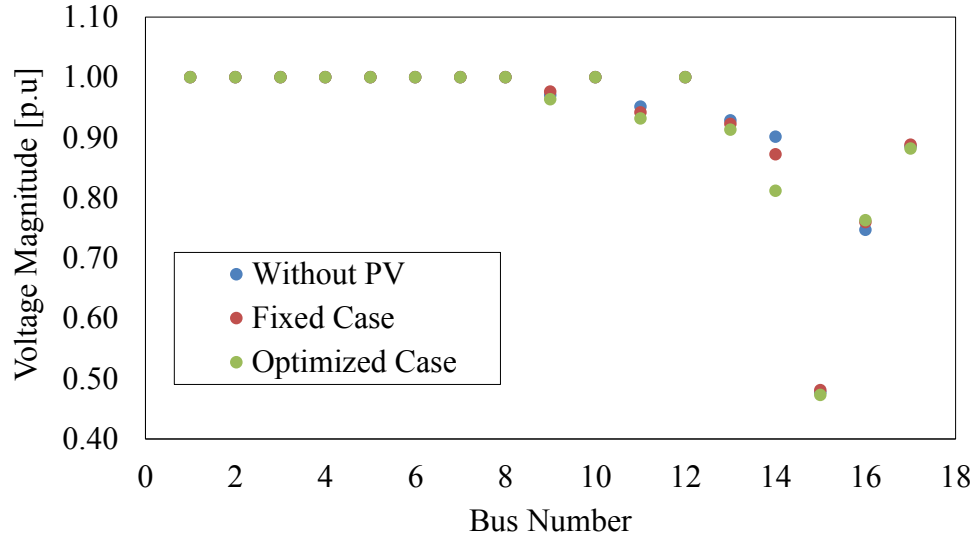


Fig. 5.14. Voltage Profile at Stability Limit (Case1 with Heavy Load)

Table 5.5: Optimal Solution in Case 1 with Heavy Load

	PV 1	PV 2	PV 3
Bus Location	8	10	12
Active Power, P_{PV} [GW]	1.579	1.834	1.952
Reactive Power, Q_{PV} [GVar]	1.532	1.215	1.015

By looking at Table 8, it can be apprehended that the solution for optimal operating points has been changed in contingency condition compared to the previous normal condition which gives big impact to power system operation.

5.3.2 Case 2 – Single Load Increase with Heavy Load

Next, the proposed method was tested in Case2 with heavy load supposing load increases only at bus 15 and 16, respectively. It is shown in Fig.39 and 40 that the similar effect with Case1 was obtained for each bus. Fig. 41 shows the voltage profile at stability limit with single load increase at bus 15.

The optimal solution in this case with single load increase at bus 15 is shown in Table 11. Reactive power output at bus 10 and 12 are the largest in this case because the voltage at the stability limit is the lowest due to the heavy power flow from generating plants to bus 15 if the DG control was not applied.

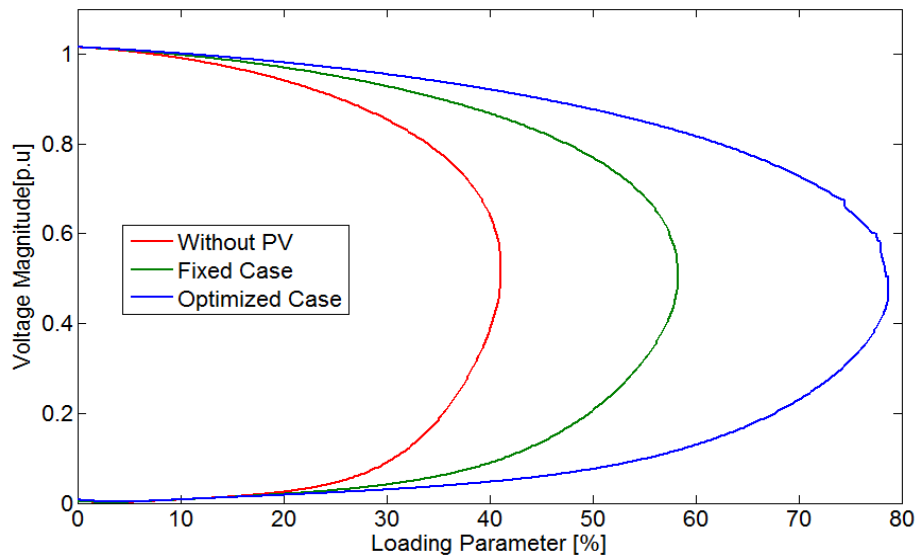


Fig. 5.15. P-V Curve at Bus 15 (Case2 with Heavy Load)

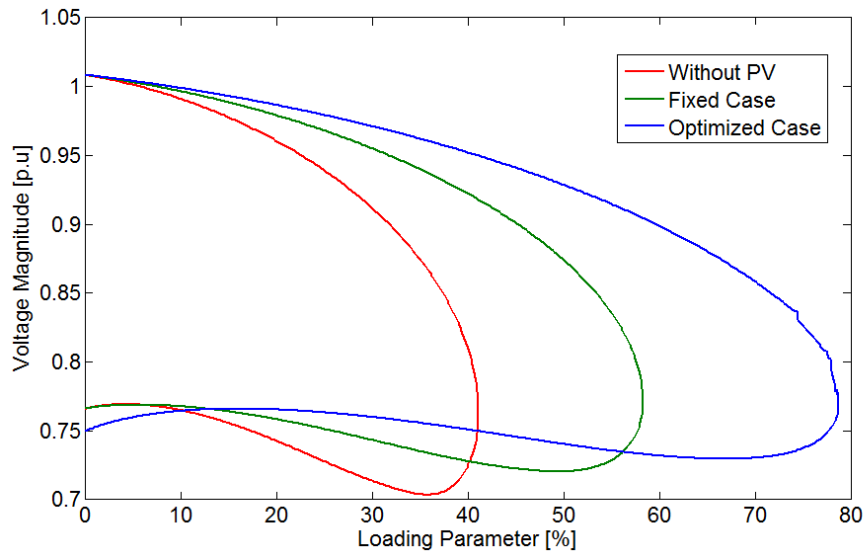


Fig. 5.16. P-V Curve at Bus 16 (Case2 with Heavy Load)

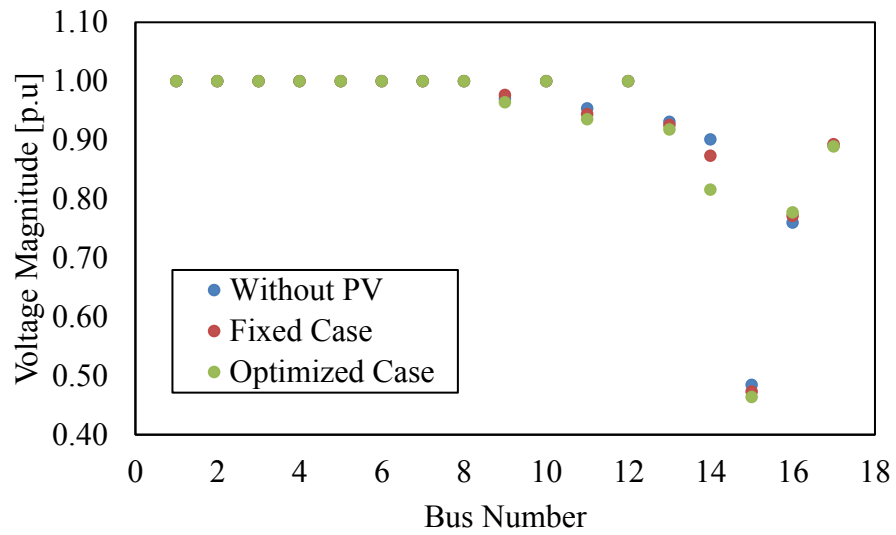


Fig. 5.17. Voltage Profile at Stability Limit with Single Load Increase at Bus 15 (Case2 with Heavy Load)

Table 5.6: Optimal Solution in Case2 with Heavy Load

	PV 1	PV 2	PV 3
Bus Location	8	10	12
Active Power, P_{PV} [GW]	1.911	1.392	1.359
Reactive Power, Q_{PV} [GVar]	1.090	1.703	1.730

Finally, the optimality of the solution was confirmed as shown in Table 12. Here, LM was recalculated with increasing or decreasing reactive power by 10 percent from the initial optimal solution. Active power is accordingly adjusted in order that the operating point moves along the circle. It is shown in this table that the proposed method properly maximizes LM.

Table 5.7: Loading Parameter Around Optimal Solution

	10% decrement	Optimal Solution	10% increment
Q_{PV1} [GVar]	0.981	1.090	1.199
Q_{PV2} [GVar]	1.532	1.703	1.873
Q_{PV3} [GVar]	1.557	1.730	1.903
Loading parameter [%]	77.72	79.27	71.28

5.3.3 Robustness of Proposed Method

A) Comparison of Proposed Method

It is more desirable that the effectiveness of the proposed method does not largely change depending on the evaluation methods. Thus, LM in Case 1 and Case 2 are compared in Fig.42. Here, bus 11, 13, 14, 15, 16 and 17 are chosen as load increase bus in Case 2. For all events, explicitly DGs incorporation establish LM at all the buses with proposed method. Here, it should be noted that the effectiveness of the proposed method can be evaluated based on the comparison between fixed and optimized approaches. Under uniform load scenario, the proposed optimized control has achieved better results than fixed control at all buses with 37.51 % of improvement.

Amongst the entire increment events in Case 2, the highest and lowest enhancements are 36.2% and 28.74% at bus 15 and bus 13, respectively. However, on average, all buses experienced improvement with applying the proposed method and its effectiveness is not largely different each other.

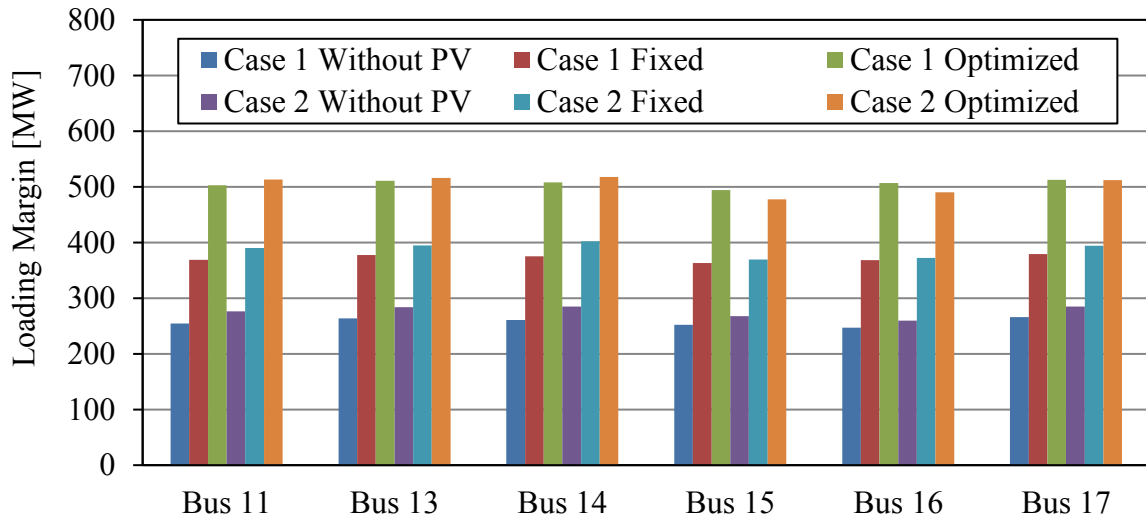


Fig. 5.18. Loading Margin in Load Buses in Case 1 and 2

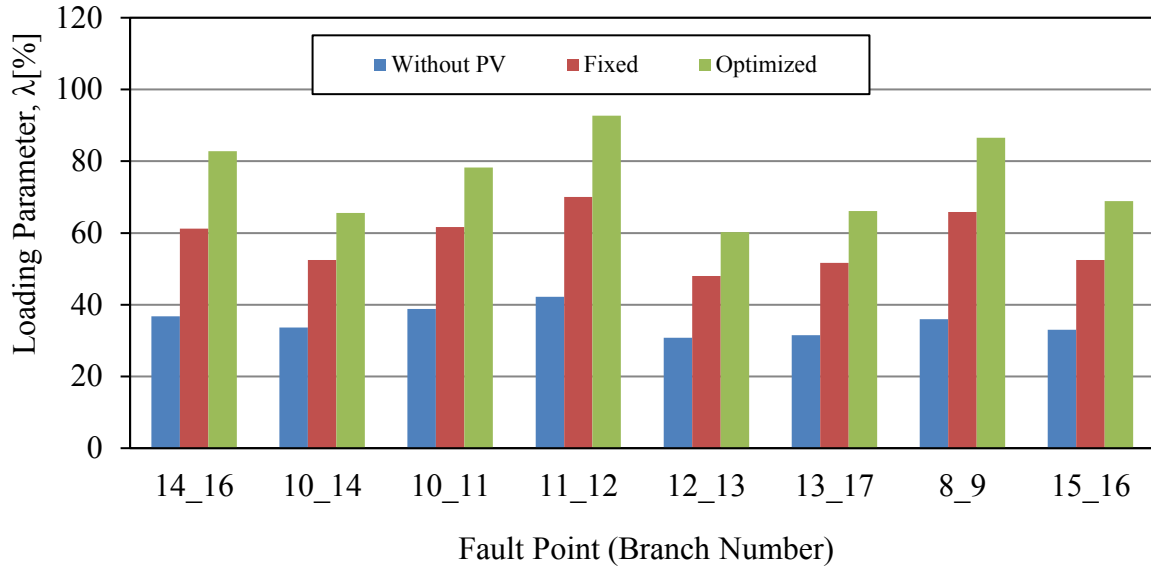


Fig. 5.19. Robustness Analysis of Fault Point

B) Robustness of Fault Conditions

In actual power system operation, the control for LM maximization should be started immediately after the fault occurrence. Therefore, the optimal control based on the assumption that fault occurs at critical branch should be used firstly because it is difficult to recalculate the optimization in short time after detecting the fault point. Thus, in this section, the robustness of the proposed method against the difference in fault point is verified.

Fig.43 shows that the LM improvement with various fault points. Here, the same optimal active and reactive power output were used in all the fault points, and the optimization was applied supposing fault occurred at transmission line 14-16. The difference between “optimized” and “fix” represents the effectiveness of the proposed method and it is expressed in percent of “fix” in this figure. The evaluation was naturally the best, 35.26%, in the case of “14-16” because the optimization technique properly works with the accurate supposition of the fault

point. Also, as for the other cases, the effectiveness was not so largely decreased. For example, in the case of “10-14”, the evaluation is 25.02% although it is the lowest enhancement. As a result, it is shown that the proposed method has robustness against fault point although it is desirable to recalculate the optimized solution after the fault point is properly detected.

Finally, in order to evaluate the computation burden of the proposed method, the convergence characteristic of PSO with single load increase at bus 15 is shown in Fig. 44. Firstly, to emphasize on reactive power drawn from PVs, we employed the number of PV one at a time until we decided to use maximum 3 number of PVs. Secondly, we reduce the presumable percentage number of total amount of PV from 60% and set to 40% of the peak demand in the MEPS model. Then, the best solutions are identified in terms of lowest fitness values and lowest average elapsed time for minimizing the power loss, voltage deviation, and curtailment. The stopping criterion is set at a maximum iteration of 300 for independent of 100 runs. We had investigated and specifically picked the values of three weight factors w , c_1 and c_2 respectively (referring to Table 1) which would have contributed to velocity and position updated in a repetitive manner until desired convergence is achieved. It is true that global optimization is not guaranteed but we tried to satisfy and neutralize it by adjusting the inertia weight, w which can be adjusted for being large, resulted in global searching and for being small resulted in the searching process becoming more local. In addition, the sum of the coefficient factor is also carefully utilized to decide the relative importance of the objectives to delineate the best optimality (i.e. $\alpha=0.2$, $\beta=0.3$ and $\gamma=0.5$). Hence, we assume from the entire adopted efforts would be sufficient and confirming the approach met its optimality with having such robustness to avoid convergence problematic as well.

In this case, the convergence has been achieved with less than 150 iterations. It is not so easy to clarify the availability of on-line operation from this result because calculation time strongly depends on the performance of CPU. In addition, the computation burden is much heavier in the actual power system operation because the scale of the network model is much larger and complicated. However, from the simulation results, we obtained here, there is a possibility that the proposed method is applicable by combining the optimization technique and control scheme as described in section 3 because the optimized solution has good robustness against the fault condition.

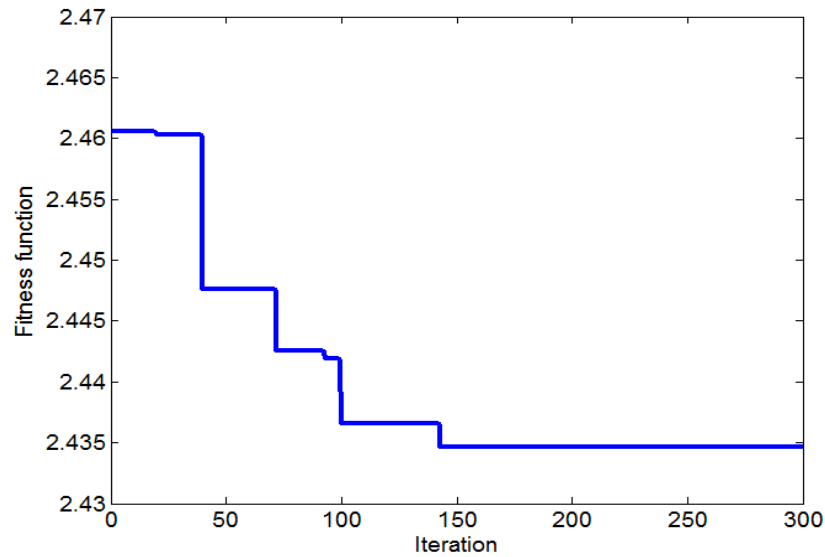


Fig. 5.20. Convergence Characteristic of PSO

It is confirmed that all the initial parameters shown in Table 3 are robust to deal under normal and contingency conditions. In fact, throughout the simulation process, MEPS model is used and successfully showed the effectiveness of the proposed method. The selections are mainly made with respect to its contributions from previous researchers (62)(63) in different kind of applications and problems. For further examination, a performance test on few different sample of problems on these parameters is conducted. It is presumed here only the number of iteration and acceleration constants (c_1 , c_2) are fixed with 300 and 2 respectively.

From Table 13, it appears that the initially selected parameters with (Population=50, w_{\max} =0.9, and w_{\min} =0.4) which were the same utilized previously in Table 6, undoubtedly outperform the others hence prominently validate the selected parameters for entire simulations conditions.

Table 5.8: Validation of PSO Parameters

Parameter	Average Fitness	Optimum Fitness
Population = 50 w_{\max} =0.9 w_{\min} =0.4	4.595	4.568
Population = 50 w_{\max} =1.4 w_{\min} =0.8	4.623	4.608
Population = 20 w_{\max} =0.9 w_{\min} =0.4	4.623	4.595
Population = 20 w_{\max} =1.4 w_{\min} =0.8	4.639	4.609

5.4 Comparison of Single and Multi-Objectives Function

It is necessary to meet both efficiency and reliability of power systems operations with regard to electricity demand whilst considering voltage stability concerns. The reactive power dispatch problem has been defined and applied to the optimization of these three objectives earlier, which are the minimization of power loss, voltage deviation, and power curtailment respectively. However, many optimization problems often confront with the

multi-objectives decision and must choose the best trade-offs for all the specified and conflicting objectives since they are lump into one. Reactive power distribution system design with Distributed Generators (DG) presence is a multi-objective problem for which it is uneasy to specify perhaps primarily due to faults and uncertainties of future demand. In this section, a comparable analysis using a single and multiple objective functions is investigated.

To be specific, here another different set of simulation environment is set up regardless pertaining directly to the previous discussion topic and the results are demonstrated well in seeking for an optimal solution. Previously from Eq. (3) the fitness function consists of three elements stated with total power loss (α) voltage deviation (β) and active power curtailment (γ). Now with rearrangement of the Eq. (3), separation of each element is normalized as in Eq. (16).

$$f(x) = F1 + F2 + F3 \quad (16)$$

To emphasize more on their contribution four cases has been simulated concurrently with the deployment of a different number of PVs installation. As opposed to previous approach the determinations of those coefficients factors is not easy so here the importance of each coefficient has been in equal from Case 1 until Case 3 except in Case 4 which arbitrarily normalized as a total summation of 1.

5.4.1 Comparison Analysis

It is shown in Table 9; a multi-objectives optimization is implemented with a different number of PVs installed. Unprecedentedly as in Table 10, a single objective function is attained consecutively associated with a subsequent number of PVs to perceived a further sense of the pragmatic. Explicitly in both tables, active power distribution is devoted thoroughly in each predetermined scenario e.g. cases and function (F).

It can be seen from Table 14 and 15 that appropriate selection of fitness or objective function must be prominent such a way to delineate decent voltage and loading margin improvement meticulously. Apart from that, optimal reactive power distributions from PV association are accommodated to uphold voltage diversification eventually. If the PV output seems larger than the PV's inverter nominal or rated capacity, then the inverter will suppress the output power from PV generators i.e. power curtailment.

Table 5.9: Multi-Objectives Optimization

Case	Parameter	1 PV	2 PV	3 PV
Case 1 ($F1$ & $F2$)	Q_{PV} , p.u	36.7172	24.9403, 27.4222	13.0583, 19.4923, 30.9828
	PV Optimal Location	7	6, 9	8, 6, 9
	$\sum P$ loss, p.u	12.2889	31.2568	51.6993
	V node, p.u	0.9910	0.9991, 1.0075	1.0094, 0.9985, 1.0053
	V dev, p.u	0.0022	0.0015	0.0031
	V critical, p.u	0.5870 at Bus 8	0.8771 at Bus 4	0.8703 at Bus 1
	Load Margin, MW	31.9488	58.3716	60.6304
Case 2 ($F1$ & $F3$)	Q_{PV} , p.u	13.5237	20.8757, 33.8762	21.7763, 18.0838, 38.2184
	PV Optimal Location	3	9, 8	5, 12, 3

	$\sum P_{\text{loss}}, \text{p.u}$	12.0192	31.2412	52.5870
	V node, p.u	0.9936	0.9929, 1.0091	1.0020, 0.9936, 1.0023
	V critical, p.u	0.5771 at Bus 6	0.5952 at Bus 4	0.8580 at Bus 7
	Load Margin, MW	34.211	53.8935	50.6862
Case 3 (F2 & F3)	$Q_{PV}, \text{p.u}$	19.9542	13.4549, 15.1031	12.7519, 14.5277, 12.5259
	PV Optimal Location	1	9, 6	12, 7, 9
	V node, p.u	0.9967	1.0091, 0.9914	0.9915, 1.0038, 0.9961
	V dev, p.u	0.0055	0.0082	0.0159
	V critical, p.u	0.6133 at Bus 4	0.5567 at Bus 4	0.9917 at Bus 8
	Load Margin, MW	33.904	51.2426	63.7743
Case 4 (F1, F2 & F3)	$Q_{PV}, \text{p.u}$	39.3509	19.3296, 17.7381	15.5908, 13.3942, 18.4839
	PV Optimal Location	10	7, 9	1, 2, 10
	$\sum P_{\text{loss}}, \text{p.u}$	12.0768	31.2500	51.7195
	V node, p.u	1.0022	0.9945, 1.0085	1.0038, 1.0040, 1.0089

	V dev, p.u	0.0005	0.0015	0.0032
	V critical, p.u	0.7953 at Bus 6	0.8651 at Bus 1	0.8217 at Bus 6
	Load Margin, MW	31.521	48.8602	51.2795

Table 5.10: Single Objective Optimization

Case	Parameter	1 PV	2 PV	3 PV
<i>F1</i>	Q_{PV} , p.u	35.7129	29.7441, 15.8088	14.8189, 38.5469, 31.8629
	PV Optimal Location	6	5, 8	9, 2, 7
	V node, p.u	1.0080	1.0019, 0.9903	0.9983, 1.0036, 1.0016
	Load Margin, MW	39.20	48.483	49.931
<i>F2</i>	Q_{PV} , p.u	18.7775	33.3922, 40.7302	15.8343, 36.7897, 29.7638
	PV Optimal Location	5	9, 6	5, 7, 3
	V node, p.u	0.9911	1.0093, 0.9943	1.0064, 0.9944, 1.0067
	Load Margin, MW	35.118	49.02	50.337
<i>F3</i>	Q_{PV} , p.u	12.5089	12.4592, 13.1395	12.6657, 15.2359, 14.2309
	PV Optimal Location	6	6, 8	5, 6, 10
	V node, p.u	0.9936	0.9997, 0.9917	0.9932, 0.9952, 0.9935
	Load Margin, MW	34.402	51.905	54.047

5.5 Summary

In this section, a decent study related to reactive power control contribution for load margin enhancement was verified. Three main topics were covered as for no DG participation and with DG participation: i-without active power curtailment and ii-with proposed method (curtailment occurs). From the simulation results, it can be deduced either for normal or contingency conditions the performances were remarkable and robust enough to be implemented in real operation but nevertheless, there was uncertain in global optimization. Therefore, sufficient effort in normalizing and confirming the proposed approach to meet ambiguous problematic was performed thoroughly. It can be concluded here load margins are improved when PVs are optimally controlled and associated with detail characteristics of the composition.

CHAPTER 6

CONCLUSION AND FUTURE WORK

6.1 Conclusion

In this thesis, the utmost aim is to investigate the potentiality of solar PV plants and its impact towards voltage stability in Malaysia power system. Knowingly, PV market in Malaysia has started in the early 1980s and it was focused on rural electrification projects. In fact, the statutory body called SEDA successfully launched and applied the implementation of Feed-in Tariff program in December 2011. Precisely the potential of this DG approach in stabilizing the operating system has urged for the country to establish the larger scale of solar power installation due to its promising potential in harvesting the resources across the nation. Furthermore, in 2015 it has been reported around 2, 845 Feed-in Approval (FiA) been approved by the authority and the largest contributor of this figures coming from solar PV. It was also claimed that RE capacity has increased by 83 % or 152 MW for annual growth hence indicates the strong determination of the key players towards achieving targeted of 2050 with RE provision in the existing power network. Admittedly three EU countries have already achieved their 2020 National Renewable Energy Action Plan (NREAP) targets namely Bulgaria, Estonia and Sweden. So, here it is determined that incorporation of solar energy will increase in time and could bring a good impact not only in supporting the country's grid voltage but also its controllability towards stabilizing the Malaysia entire power system transfer regionally.

Undoubtedly, it is of prime importance to keep voltage stability to avoid large-scale blackout caused by voltage collapse. To this end, the effectiveness of reactive power support by DG was studied with developing a maximization method of LM based on optimization technique. Both normal and contingency conditions were treated in the proposed method considering the trade-off relationship between reactive power control and active power curtailment. Through numerical simulations by using MEPS model, it was shown that the proposed method could maximize LM with good robustness against the uncertainty of the fault cases. It is expected that the voltage profile of the network can be well-maintained with maximizing LM by giving the optimal reference value with decentralized control considering voltage constraint as described in section 3.

6.2 Future Work

Although the proposed method has achieved the desired research objectives, yet the areas of the future works can be carried out to urge more significant enhancement as follows:

- i. The maximum reactive power output from DG also depends on the terminal voltage of the DG because of the current limit of PCS. In particular, this effect should be taken into account when DGs are located at the critical bus whose voltage becomes very low under contingency condition.
- ii. The effectiveness of the proposed method will be verified by using other network models with a different impedance ratio of transmission lines.
- iii. Only constant power loads are used in this paper. The load model should be improved with considering induction motors.

LIST OF PUBLICATION

JOURNAL

1. N. Bin Salim, T. Tsuji, T. Oyama, and K. Uchida, "Optimal Control of Solar Energy Resources in Loading Margin Enhancement for Peninsular Malaysia Network using Artificial Neural Network (ANN) Model," *Applied Mechanics and Materials*, Vol. 785, pp. 606-607, 2015.
2. Norhafiz SALIM, T. Tsuji, T. Oyama, and K. Uchida, "Optimal Reactive Power Control of Inverter-Based Distributed Generator for Voltage Stability Insight using Particle Swarm Optimisation," *IEEJ Transaction on Power and Energy*, Vol.137, No.5, 2017

PROCEEDING

1. Norhafiz Bin Salim, Takao TSUJI, Tsutomu OYAMA, and Kenko UCHIDA, "Optimal Operation and Planning Using FACTS Devices in Power Systems with PV Generators," *Solar Integration Workshop (SIW) 2014*, Berlin, Germany.
2. N. Bin Salim, T. Tsuji, T. Oyama "Loading Margin Estimation in Malaysia Power System with PV Generator using Statistical Models : Artificial Neural Networks," in *IEJ Technical Meeting*, 24 March 2015, Japan, pp. 1–2.
3. N. Bin Salim, T. Tsuji, T. Oyama, and K. Uchida, "Optimal Control of Solar Energy Resources in Loading Margin Enhancement for Peninsular Malaysia Network using Artificial Neural Network (ANN) Model," in *Int. Power Engineering and Optimization Conference (PEOCO)*, 18-20 March 2015, Malaysia pp. 1–5.
4. N. B. Salim, T. Tsuji, T. Oyama, and K. Uchida "Fast Method for Loading Margin Classification in Voltage Stability Analysis for Malaysia Power Network With Solar Provision And N-1 Criterion," in *Int. Conf. on Electrical Engineering (ICEE)*, 5-9 July 2015, Hong Kong, pp. 1–6.

5. N. B. Salim, T. Tsuji, T. Oyama, and K. Uchida “Interface Flow Limit Identification Using Focused Time Delay Network for MEPS Transmission,” in *IEEE PES, Innovative Smart Grid Technologies (ISGT)*, 4-6 November 2015, Thailand, pp. 1–6.
6. N. B. Salim, T. Tsuji, T. Oyama, and K. Uchida “A Reactive Power Control Strategy for Preventing Voltage Collapse for Malaysian Power Network with Multiple Photovoltaic Plants,” in *Solar Integration Workshop (SIW 2015)*, 19-20 October 2015, Brussels, Belgium, pp. 1–6.
7. N. B. Salim, T. Tsuji, T. Oyama, and K. Uchida “Comparison of Single and Multi-Objectives for Optimal DGs Reactive Power Dispatch using PSO,” in *IEEE PES, Innovative Smart Grid Technologies (ISGT)*, 28 November - 1 December 2016, Melbourne, Australia, pp. 1–6.
8. Norhafiz Bin SALIM, Hossam ABOELSOUND, Takao TSUJI, Tsutomu OYAMA, and Kenko UCHIDA, “Load Frequency Control of Two-Area Network using Renewable Energy Resources and Battery Energy Storage System,” in *Int. Power Engineering and Optimization Conference (PEOCO)*, 8-9 April 2017, Malaysia pp. 1–8.

REFERENCES

- (1) M. Cimino and P. R. Pagilla, "Reactive Power Control for Multiple Synchronous Generators Connected in Parallel," no. 99, pp. 1–8, 2016.
- (2) Y. Miao and H. Cheng, "An Optimal Reactive Power Control Strategy for UHVAC/DC Hybrid System in East China Grid," *IEEE Trans. Smart Grid*, vol. 7, no. 1, pp. 1–8, 2014.
- (3) E. Demirok, P. C. González, K. H. B. Frederiksen, D. Sera, P. Rodriguez, and R. Teodorescu, "Local Reactive Power Control Methods for Overvoltage Prevention of Distributed Solar Inverters in Low-Voltage Grids," *IEEE J. Photovoltaics*, vol. 1, no. 2, pp. 174–182, 2011.
- (4) B. Tamimi, C. A. Cañizares, and S. Vaez-Zadeh, "Effect of Reactive Power Limit Modeling on Maximum System Loading and Active and Reactive Power Markets," *IEEE Trans. Power Syst.*, vol. 25, no. 2, pp. 1106–1116, 2010.
- (5) F. Dong, B. H. Chowdhury, M. L. Crow, and L. Acar, "Improving Voltage Stability by Reactive Power Reserve Management," *IEEE Trans. Power Syst.*, vol. 20, no. 1, pp. 338–345, 2005.
- (6) F. A. Viawan and D. Karlsson, "Voltage and Reactive Power Control in Power Systems with Synchronous Machine Based Distributed Generation," *IEEE Trans. Power Deliv.*, vol. 23, no. 2, pp. 1079–1087, 2008.
- (7) Yasuji Sekine and H. Ohtsuki, "Cascaded Voltage Collapse," *IEEE Trans. Power Syst.*, vol. 5, no. 1, pp. 250–256, 1990.
- (8) J. F. Zhang, C. T. Tse, W. Wang, and C. Y. Chung, "Voltage Stability Analysis Based on Probabilistic Power Flow and Maximum Entropy," *IET Gener. Transm. Distrib.*, vol. 4, no. 4, pp. 530–537, 2010.

- (9) I. Dobson and L. Lu, "Voltage Collapse Precipitated by the Immediate Change in Stability when Generator Reactive Power Limits are Encountered," *IEEE Trans. Circuits Syst.*, vol. 39, no. 9, pp. 762–766, 1992.
- (10) B. K. Turitsyn, M. Ieee, S. Backhaus, and M. Chertkov, "Options for Control of Reactive Power by Distributed Photovoltaic Generators," vol. 99, no. 6, pp. 1063–1073, 2011.
- (11) E. Demirok, P. C. Gonz, K. H. B. Frederiksen, D. Sera, P. Rodriguez, and R. Teodorescu, "Local Reactive Power Control Methods for Overvoltage Prevention of Distributed Solar Inverters in Low-Voltage Grids," *IEEE J. Photovoltaics*, vol. 1, no. 2, pp. 174–182, 2011.
- (12) B. B. Zad, J. Lobry, F. Vallee, and H. Hasanvand, "Optimal Reactive Power Control of DGs for Voltage Regulation of MV Distribution Systems Considering Thermal Limit of the System Branches," *Int. Conf. Power Syst. Technol. Towar. Green, Effic. Smart Power Syst. Proc.*, pp. 2951–2958, 2014.
- (13) S. Deshmukh, B. Natarajan, and A. Pahwa, "Voltage / VAR Control in Distribution Networks via Reactive Power Injection Through Distributed Generators," *IEEE Trans. Smart Grid*, vol. 3, no. 3, pp. 1226–1234, 2012.
- (14) A. Camacho, M. Castilla, J. Miret, R. Guzman, and A. Borrell, "Reactive Power Control for Distributed Generation Power Plants to Comply with Voltage Limits During Grid Faults," *IEEE Trans. Power Electron.*, vol. 29, no. 11, pp. 6224–6234, 2014.
- (15) X. Su, M. A. S. Masoum, and P. J. Wolfs, "Optimal PV Inverter Reactive Power Control and Real Power Curtailment to Improve Performance of Unbalanced Four-wire LV Distribution networks," *IEEE Trans. Sustain. Energy*, vol. 5, no. 3, pp. 967–977, 2014.

- (16) S. Adhikari and F. Li, "Coordinated V-f and P-Q Control of Solar Photovoltaic Generators With MPPT and Battery Storage in Microgrids," *IEEE Trans. Smart Grid*, vol. 5, no. 3, pp. 1270–1281, 2014.
- (17) X. Liu, A. Aichhorn, L. Liu, and H. Li, "Coordinated Control of Distributed Energy Storage System with Tap Changer Transformers for Voltage Rise Mitigation Under High Photovoltaic Penetration," *IEEE Trans. Smart Grid*, vol. 3, no. 2, pp. 897–906, 2012.
- (18) P. Jahangiri and D. C. Aliprantis, "Distributed Volt/VAr Control by PV Inverters," *IEEE Trans. Power Syst.*, vol. 28, no. 3, pp. 3429–3439, 2013.
- (19) T. Case, B. Tamimi, C. Cañizares and K. Bhattacharya, "System Stability Impact of Large-Scale and Distributed Solar Photovoltaic Generation :," *IEEE Trans. Sustain. Energy*, vol. 4, no. 3, pp. 680–688, 2013.
- (20) C. M. Shen and M. A. Laughton, "Power-System Load Scheduling with Security Constraints using Dual Linear Programming," *Proc. Inst. Electr. Eng.*, vol. 117, no. 11, pp. 2117–2127, 1970.
- (21) L. C. A. Ferreira, A. C. Z. De Souza, S. Granville, and J. W. M. Lima, "Interior Point Method Applied to Voltage Collapse Problems and System Losses Reduction," *IEE Proc. - Gener. Transm. Distrib.*, vol. 149, no. 2, pp. 165–170, 2002.
- (22) W. Yan, S. Lu, and D. C. Yu, "A Novel Optimal Reactive Power Dispatch Method Based on an Improved Hybrid Evolutionary Programming Technique," *IEEE Trans. Power Syst.*, vol. 19, no. 2, pp. 913–918, 2004.
- (23) Y. C. Chang, "Multi-Objective Optimal SVC Installation for Power System Loading Margin Improvement," *IEEE Trans. Power Syst.*, vol. 27, no. 2, pp. 984–992, 2012.

- (24) M. Parniani, M. Parvania, A. Rabiee, M. Fotuhi-Firuzabad, and M. Vanouni, "Comprehensive Control Framework for Ensuring Loading Margin of Power Systems Considering Demand-Side Participation," *IET Gener. Transm. Distrib.*, vol. 6, no. 12, pp. 1189–1201, 2012.
- (25) A. Rabiee and M. Parniani, "Voltage Security Constrained Multi-Period Optimal Reactive Power Flow using Benders and Optimality Condition Decompositions," *IEEE Trans. Power Syst.*, vol. 28, no. 2, pp. 696–708, 2013.
- (26) S. Mishra, "Bacteria Foraging-Based Solution to Optimize Both Real Power Loss and Voltage Stability Limit," *2007 IEEE Power Eng. Soc. Gen. Meet. PES*, vol. 22, no. 1, pp. 240–248, 2007.
- (27) Y. Xu, Z. Y. Dong, C. Xiao, R. Zhang, and K. P. Wong, "Optimal Placement of Static Compensators for Multi-Objective Voltage Stability Enhancement of Power Systems," *IET Gener. Transm. Distrib.*, vol. 9, no. 15, pp. 2144–2151, 2015.
- (28) A. Sode-Yome, N. Mithulananthan, and K. Y. Lee, "A Maximum Loading Margin Method for Static Voltage Stability in Power Systems," *IEEE Trans. Power Syst.*, vol. 21, no. 2, pp. 799–808, 2006.
- (29) H. A. Shayanfar, H. Razmi, and M. Teshnehlab, "Neural Network based on a Genetic Algorithm for Power System Loading Margin Estimation," *IET Gener. Transm. Distrib.*, vol. 6, no. 11, pp. 1153–1163, 2012.
- (30) G. Catalina, A. Gomez and W. Vargas, "Computation of Maximum Loading Points via the Factored Load Flow," *IEEE Trans. Power Syst.*, vol. 31, no. 5, pp. 4128–4135, 2016.
- (31) H. Y. Su and C. W. Liu, "Estimating the Voltage Stability Margin Using PMU Measurements," *IEEE Trans. Power Syst.*, vol. 31, no. 4, pp. 3221–3229, 2016.

- (32) T. Zabaoui, L.-A. Dessaint, and I. Kamwa, "Preventive Control Approach for Voltage Stability Improvement using Voltage Stability Constrained Optimal Power Flow based on Static Line Voltage Stability Indices," *IET Gener. Transm. Distrib.*, vol. 8, no. 5, pp. 924–934, 2014.
- (33) E. Haesen, C. Bastiaensen, J. Driesen, and R. Belmans, "A Probabilistic Formulation of Load Margins in Power Systems with Stochastic Generation," *IEEE Trans. Power Syst.*, vol. 24, no. 2, pp. 951–958, 2009.
- (34) F. C. V Malange, D. A. Alves, L. C. P. da Silva, C. A. Castro, and G. R. M. da Costa, "Real Power Losses Reduction and Loading Margin Improvement via Continuation Method," *IEEE Trans. Power Syst.*, vol. 19, no. 3, pp. 1690–1692, 2004.
- (35) Y. Zhou and V. Ajjarapu, "A Fast Algorithm for Identification and Tracing of Voltage and Oscillatory Stability Margin Boundaries," *Proc. IEEE*, vol. 93, no. 5, pp. 934–946, 2005.
- (36) D. Zhou, "Online monitoring of Voltage Stability Margin Using An Artificial Neural Network," *Power Syst. IEEE ...*, vol. 25, no. 3, pp. 1566–1574, 2010.
- (37) L. Wang and H. D. Chiang, "Toward Online Line Switching for Increasing Load Margins to Static Stability Limit," *IEEE Trans. Power Syst.*, vol. 31, no. 3, pp. 1744–1751, 2016.
- (38) S. Mahapatra, A. N. Jha, and B. K. Panigrahi, "Hybrid Technique for Optimal Location and Cost Sizing of Thyristor Controlled Series Compensator to Upgrade Voltage Stability," vol. 75, no. 3, pp. 1–7, 2016.
- (39) Y. Dong, X. Xie, B. Zhou, W. Shi, and Q. Jiang, "An Integrated High Side Var-Voltage Control Strategy to Improve Short-Term Voltage Stability of Receiving-End Power Systems," *IEEE Trans. Power Syst.*, vol. 31, no. 3, pp. 2105–2115, 2016.

- (40) N. C. Hien, N. Mithulananthan, and R. C. Bansal, "Location and Sizing of Distributed Generation Units for Loadability Enhancement in Primary Feeder," *IEEE Syst. J.*, vol. 7, no. 4, pp. 797–806, 2013.
- (41) A. Rabiee, A. Soroudi, and B. Mohammadi-ivatloo, "Corrective Voltage Control Scheme Considering Demand Response and Stochastic Wind Power," vol. 29, no. 6, pp. 2965–2973, 2014.
- (42) D. Jia, L. Hu, K. Liu, Y. Liu, X. Meng, and W. Sheng, "Simplified Probabilistic Voltage Stability Evaluation Considering Variable Renewable Distributed Generation in Distribution Systems," *IET Gener. Transm. Distrib.*, vol. 9, no. 12, pp. 1464–1473, 2015.
- (43) M. H. Hemmatpour, M. Mohammadian, and A. A. Gharaveisi, "Simple and Efficient Method for Steady-State Voltage Stability Analysis of Islanded Microgrids with Considering Wind Turbine Generation and Frequency Deviation," *IET Gener. Transm. Distrib.*, vol. 10, no. 7, pp. 1691–1702, 2016.
- (44) S. Patra, D. Chatterjee, and S. Konar, "V–Q Sensitivity-Based Index for Assessment of Dynamic Voltage Stability of Power Systems," *IET Gener. Transm. Distrib.*, vol. 9, no. 7, pp. 677–685, 2015.
- (45) M. F. Zambroni de Souza, Y. Reis, A. B. Almeida, I. Lima, and A. C. Zambroni de Souza, "Load Margin Assessment of Systems with Distributed Generation with the Help of A Neuro-Fuzzy Method," *IET Renew. Power Gener.*, vol. 9, no. 4, pp. 331–339, 2015.
- (46) M. Ravilla and G. Ramamohan Rao, "Modeling and Simulation of a Distribution STATCOM for Power Quality Problems-Voltage Sag and Swell based on SPWM," *IEEE Int. Conf. Advance. Engineering. Science and Management*, pp. 436–441, 2012.

- (47) K. Mahesh, P. Al Nallagownden, and I. Al Elamvazuthi, "Optimal Placement and Sizing of DG in Distribution System using Accelerated PSO for Power Loss Minimization," *2015 IEEE Conf. Energy Conversion, CENCON 2015*, pp. 193–198, 2016.
- (48) D. Q. Hung and N. Mithulanathan, "Multiple distributed generator placement in primary distribution networks for loss reduction," *IEEE Trans. Ind. Electron.*, vol. 60, no. 4, pp. 1700–1708, 2013.
- (49) A. Ameli, S. Bahrami, F. Khazaeli, and M. R. Haghifam, "A multiobjective particle swarm optimization for sizing and placement of DGs from DG owner's and distribution company's viewpoints," *IEEE Trans. Power Deliv.*, vol. 29, no. 4, pp. 1831–1840, 2014.
- (50) Shertukde, H.M. *Distributed Photovoltaic Grid Transformers*. Taylor & Francis Group.
- (51) <http://www.seda.gov.my>
- (52) <http://www.mbipv.net.my>
- (53) Ir. Ahmad H.H and Julian D. (2009) *The Final Report on The Renewable Energy Policy & Action Plan*. www.mbipv.com.
- (54) "Recommended Practice for Simulation Models for Automatic Generation Control," *IEEJ Technical Report*, no. 1386, December 2016.
- (55) Tamer Khatib, Azah Mohamed, K.Sopian and M. Mahmoud "Solar Energy Prediction for Malaysia Using Artificial Neural Networks," *Int. Journal of Photoenergy*, vol. 2012, no. 4, pp. 1-16, 2012.

- (56) J. Kennedy and R. Eberhart, "Particle Swarm Optimization," *Neural Networks, Proceedings., IEEE Int. Conf.*, vol. 4, pp. 1942–1948, 1995.
- (57) P. Kundur, "Power System Stability and Control." McGraw-hill, 1994.
- (58) A.Saed and W.M. Wan Kadir," Applying Particle Swarm Optimization to Software Performance Prediction- An Introduction to the Approach," 5th Malaysian Conf. Softw. Eng. MySEC,pp.207-212, 2011.
- (59) M. Hassan and M. Abido, "Optimal Design of Microgrids in Autonomous and Grid-Connected Modes Using Particle Swarm Optimization," *IEEE Trans. Power Electron.*, vol. 26, no. 3, pp. 755–769, 2011.
- (60) S. A. Sulaiman, M. N. H. Mat, F. M. Guangul, and M. A. Bou-Rabee, "Real-time Study on the Effect of Dust Accumulation on Performance of Solar PV Panels in Malaysia," *Int. Conf. Electr. Inf. Technol.*, pp. 269–274, 2015.
- (61) Department of Energy Management and Industry, "Electricity Supply Industry: Performance and Statistical Information 2010," *www.st.gov.my*, pp. 1–103, 2010.
- (62) S. Xianchao, T. Yufei, H. Haibo, and W. Jinyu, "Energy-Storage-Based Low-Frequency Oscillation Damping Control Using Particle Swarm Optimization and Heuristic Dynamic Programming," *IEEE Trans. Power Syst.*, vol. 29, no. 5, pp. 2539–2548, 2014.
- (63) F. R. Durand, V. D. Bacon, S. A. Oliveira da Silva, L. P. Sampaio, F. M. de Oliveira, and L. B. G. Campanhol, "Grid-tied Photovoltaic System Based on PSO MPPT Technique with Active Power Line Conditioning," *IET Power Electron.*, vol. 9, no. 6, pp. 1180–1191, 2016.

APPENDIX A

Line impedance of transmission lines in the MEPS model is shown in Table A with the base capacity of 100MVA.

Bus number		Line Impedance [p.u]		
From	To	R	X	B/2
12	4	0	0.010212	0
10	5	0	0.010212	0
9	6	0	0.010212	0
17	2	0	0.010212	0
15	8	0.004201	0.032541	0.0312
9	10	0.003144	0.026513	0.0192
11	10	0.005144	0.036513	0.0192
14	9	0.005144	0.036513	0.0312
12	11	0.004201	0.03254	0.0192
7	8	0	0.010212	0
16	17	0.004201	0.032541	0.0192
12	13	0.003144	0.026513	0.0312
14	16	0.004201	0.03254	0.0118
15	16	0.003144	0.026513	0.0118
1	16	0	0.010212	0
13	17	0.003144	0.026513	0.0018
9	8	0.004201	0.032541	0.0192
13	3	0	0.010212	0

APPENDIX B



Fig. C1. Peninsular Malaysia Grid System

Source:

http://www.geni.org/globalenergy/library/national_energy_grid/malaysia/malaysiannationalelectricitygrid.shtml55